

UNIVERSITA` DEGLI STUDI DI PADOVA

Dipartimento di Scienze del Farmaco

Master Degree in Pharmaceutical Biotechnology

Final Dissertation

On

*“Characterisation and Mechanism of Action Investigation of
Novel Rhenium-containing Antibiotics”*

Thesis Supervisor

Prof. Stefano Comai

Candidate

Shubhda Dev

External Supervisor

Dr. Michaela Wenzel

Academic Year 2023/24

Acknowledgement

I would like to express my deepest gratitude to Dr. Michaela Wenzel, Associate Professor, Department of Life Sciences, Chalmers University of Technology, for giving me the opportunity to work on this significant project and for the constant feedback and support.

I am immensely thankful to Professor Stefano Comai, Associate Professor of Pharmacology, Department of Pharmaceutical and Pharmacological Sciences, University of Padova, for his invaluable supervision throughout the project.

I would like to thank Dr. Gabriela M. Righetto for her guidance, patience, and input throughout the project and for teaching me so amazingly.

I would like to acknowledge and extend my gratitude to the members of the Wenzel lab for fostering a positive and collaborative working environment.

Thanks to Rahul, Guna, Harshwardhan, Manisha, Arup, and Yogeshwar for their valuable academic inputs throughout this course.

Finally, I would like to thank my parents for their love, constant encouragement and for letting me follow my passion. Thanks to my loving brother for being a pillar of strength for me.

Table of Contents

<i>Abstract</i>	10
<i>Chapter 1</i>	12
Introduction	12
1. What is Antimicrobial Resistance or Multi Drug resistance?.....	12
2. Background and Significance of Antimicrobial Resistance.....	13
3. Metal Complexes in Antibacterial Research.....	14
3.1 Metal Complexes and their potential as Antibacterial agents.....	15
3.2 Historical context and development of Metal based Antibiotics	16
4. Mechanism of Action.....	16
4.1 How Metal complexes exert antibacterial effect?	16
4.1.1 Disruption of Cell Membrane Integrity :.....	17
4.1.2 Reactive Oxygen Species (ROS) Generation :.....	18
4.1.3 Chelation of Essential Metals :	19
4.1.4 Inhibition of Enzymatic Activity :	19
5. Effectiveness of metal complexes against MDR strains	20
5.1 Performance Comparison to conventional Antibiotics	21
5.1.2 Resistance Mechanisms :.....	21
5.1.3 Safety :.....	21
<i>Chapter 2</i>	22
Scope of the study	22
1. Rationale of the Thesis	22
1.1 Why Rhenium Complex?	23
1.2 Antibiotics.....	24
1.3 Experimental Assays:	25
<i>Chapter 3</i>	28
Materials and Methods	28
1. Minimal Inhibitory Concentration	28
2. Growth curve	30
3. DiSC ₃ (5)	32
4. Bacterial cytological profiling (BCP).....	34
5. Protein localization study.....	36
6. Single Molecule Localization Imaging.....	38
<i>Chapter 4</i>	42
Results and Discussions	42
1. Minimal Inhibitory Concentration	42
2. Growth Curve	43
3. DiSC ₃ (5)Diffusion Assay.....	46
4. Bacterial Cytological Profiling	48
5. Protein Localization assay	52
5.1 MinD localization	52
5.2 RecA localization	54
5.3 MreB localization	55
5.4 DnaN localization	57
5.4 YocM localization	59
6. Single Molecule Localization Imaging.....	60
<i>Conclusions</i>	62
<i>References</i>	64

List of Tables

TABLE 1 ANTIBIOTICS USED IN THIS STUDY, THEIR KNOWN TARGET AND THEIR INTRACELLULAR MECHANISM OF ACTION IN BACTERIAL CELLS	24
TABLE 2 COMPONENTS IN LB MEDIA	28
TABLE 3 B. SUBTILIS AND GENOTYPES USED FOR PROTEIN LOCALIZATION ASSAY AND INDUCER CONCENTRATIONS USED FOR EACH STRAIN.....	37
TABLE 4 ENZYMES USED AND THEIR FUNCTIONS.....	38
TABLE 5 THE ENZYMES USED FOR DNA DAMAGE LABELLING AND THE CORRESPONDING CONCENTRATIONS.....	39
TABLE 6 THE NUCLEOTIDES USED FOR DNA DAMAGE LABELLING AND THE CORRESPONDING CONCENTRATIONS	40

List of Figures

FIGURE 1. STRUCTURE OF RE1	22
FIGURE 2. STRUCTURE OF RE4	22
FIGURE 3. 96-WELL MICROTITER PLATE PREPARATION FOR THE DETERMINATION OF MINIMAL INHIBITORY CONCENTRATION. THE E IN THE MICROTITER PLATE DENOTES STERILE CONTROL AND GC IS THE GROWTH CONTROL. THE VALUES ARE IN MM AND DENOTES THE REDUCING CONCENTRATION OF COMPOUNDS.	29
FIGURE 4. 96-WELL MICROTITER PLATE ASSEMBLY TO DETERMINE THE GROWTH CURVE USING ABSORBANCE SPECTROPHOTOMETRY WHERE ROW A CONTAINS RE1 WHEREAS ROW B CONTAINS RE4. THE E IN THE MICROTITER PLATE DENOTES STERILE CONTROL AND GC IS THE GROWTH CONTROL.....	31
FIGURE 5. MEMBRANE DEPOLARIZATION ASSAY WITH DISC3(5). THE DYE ACCUMULATES AT THE POLARIZED MEMBRANE AND IS RELEASED WHEN THE CELL DEPOLARIZES. THE RELEASE OF THE DYE RESULTS IN AN INCREASED FLUORESCENCE SIGNAL (SCHÄFER AND WENZEL, 2020).	32
FIGURE 6. 96-WELL PLATE ASSEMBLY FOR THE MEASUREMENT OF FLUORESCENCE WITH DISC3(5) WHERE ROW A REPRESENTS CONCENTRATIONS OF RE1 AND ROW B REPRESENTS CONCENTRATION OF RE4 USED TO TREAT CELLS. GM REPRESENTS GRAMICIDIN USED AS A POSITIVE CONTROL. THE 6TH WELL DENOTES UNTREATED CELLS AND THE 7TH WELL CONTAINS ONLY COMPOUNDS AND MEDIUM.	33
FIGURE 7. GROWTH CURVE FOR RE1 WITH DIFFERENT CONCENTRATION OF RE1 ADDED TO CELLS. GC DENOTES THE GROWTH CONTROL WHICH DOES NOT CONTAIN RE1 COMPOUND	43
FIGURE 8. GROWTH CURVE FOR RE1 WITH DIFFERENT CONCENTRATION OF RE1 ADDED TO THE CELLS. GC DENOTES THE GROWTH CONTROL WHICH DOES NOT CONTAIN RE1 COMPOUND	43
FIGURE 9. GROWTH CURVE FOR RE4 WITH DIFFERENT CONCENTRATION OF RE4 ADDED TO THE CELLS. GC DENOTES THE GROWTH CONTROL WHICH DOES NOT CONTAIN RE4 COMPOUND	45

FIGURE 10. GROWTH CURVE FOR RE4 WITH DIFFERENT CONCENTRATIONS OF RE4 ADDED TO THE CELLS. GC DENOTES THE GROWTH CONTROL AND DOES NOT CONTAIN RE4 COMPOUND45

FIGURE 11. DISC₃(5) DIFFUSION ASSAY FOR RE1.....46

FIGURE 12. DISC₃(5) DIFFUSION ASSAY FOR RE4.....47

FIGURE 13. BACTERIAL CYTOLOGICAL PROFILING OF MW54 CELLS USING RE1 WITH NILE RED, GFP AND DAPI STAINS.....48

FIGURE 14. BACTERIAL CYTOLOGICAL PROFILING OF MW54 USING RE4 WITH NILE RED, GFP AND DAPI STAINS49

FIGURE 15. NUCLEOID COMPACTION MEASUREMENT FOR RE1 WITH A MACRO DEVELOPED BY GRIMSHAW. MEASUREMENTS WERE DONE USING DAPI CHANNEL OF THE BCP EXPERIMENT OF 3 BIOLOGICAL REPLICATES. NUCLEOID COMPACTION WAS CALCULATED BY THE RATIO OF CELL AREA AND DNA AREA. A LOW VALUE CORRESPONDS TO A RELAXED NUCLEOID, WHILE A HIGH VALUE INDICATES HIGHER DNA COMPACTION. THE MEDIAN OF THE NEGATIVE CONTROL IS INDICATED WITH A DASHED RED LINE. THE BLACK DASH INDICATES THE MEDIAN OF THE DATA SET. STATISTICAL SIGNIFICANCE WAS CONDUCTED USING A TWO-TAILED STUDENT’S T-TEST ($P \leq 0,05$).....50

FIGURE 16. NUCLEOID COMPACTION MEASUREMENT FOR RE4 WITH A MACRO DEVELOPED BY GRIMSHAW. MEASUREMENTS WERE DONE USING DAPI CHANNEL OF THE BCP EXPERIMENT OF 3 BIOLOGICAL REPLICATES. NUCLEOID COMPACTION WAS CALCULATED BY THE RATIO OF CELL AREA AND DNA AREA. A LOW VALUE CORRESPONDS TO A RELAXED NUCLEOID, WHILE A HIGH VALUE INDICATES HIGHER DNA COMPACTION. THE MEDIAN OF THE NEGATIVE CONTROL IS INDICATED WITH A DASHED RED LINE. THE BLACK DASH INDICATES THE MEDIAN OF THE DATA SET. STATISTICAL SIGNIFICANCE WAS CONDUCTED USING A TWO-TAILED STUDENT’S T-TEST ($P \leq 0,05$).....51

FIGURE 17. MIND LOCALIZATION FOR RE1 USING GFP52

FIGURE 18. MIND LOCALIZATION FOR RE4 USING GFP53

FIGURE 19. MIND LOCALIZATION FOR RE4(5 MINUTE ANTIBIOTIC TREATMENT) USING GFP	53
.....	
FIGURE 20. RECA LOCALIZATION FOR RE1 USING GFP	54
FIGURE 21. RECA LOCALIZATION FOR RE4 USING GFP	55
FIGURE 22. MREB LOCALIZATION FOR RE1 USING GFP	56
FIGURE 23. MREB LOCALIZATION FOR RE4 USING GFP	57
FIGURE 24. DNAN LOCALIZATION FOR RE1 USING GFP AND DAPI	58
FIGURE 25. DNAN LOCALIZATION FOR RE4 USING GFP AND DAPI	58
FIGURE 26. YOCCM LOCALIZATION FOR RE1 USING GFP	59
FIGURE 27 YOCCM LOCALIZATION FOR RE4 USING GFP	60
FIGURE 28 HIGHEST AND LOWEST CONCENTRATION OF RE1 AND RE4 TO PERFORM SINGLE MOLECULE IMAGING TO CHECK DNA DAMAGE REPAIR	61

Abbreviations

Re Rhenium

AMR Antimicrobial Resistance

APTES Aminopropyltriethoxysilane

ATMS Allyltrimethoxysilane

BCP bacterial cytological profiling

BSA Bovine Serum Albumin

Cip ciprofloxacin

Van Vancomycin

Mit Mitomicin

MIC Minimum Inhibitory Concentration

DAPI 4',6-diamidino-2-phenylindole

DISC3(5) [3,3'-Dipropylthiadicarbocyanine iodide]

DMSO dimethyl sulfoxide

DNA deoxyribonucleic acid

DSBs DNA double-strand breaks

EDTA Ethylenediaminetetraacetic acid

GFP green-fluorescent protein

LB luria-bertani

OD optical density

OSC optimal stressor concentration

PBS phosphate-buffered saline

PI Propidium Iodide

RNA ribonucleic acid

RPM rounds per minute

Abstract

Antimicrobial resistance (AMR) poses a significant global threat to public health, necessitating innovative strategies to combat the rise of multidrug-resistant pathogens. This thesis investigates the use of two novel Rhenium-complexed antibiotic derivatives as potential antimicrobials to address the challenges associated with antibiotic resistance. The research involves a comparison study, examining the behaviour of bacteria under varying concentrations of these rhenium complexes.

The study employs a range of analytical techniques, including Minimal Inhibitory Concentration (MIC) assays, Growth curve analysis, Bacterial Cytological Profiling (BCP) and Protein Localization studies by performing single cell fluorescence imaging, DiSC₃(5) diffusion assay, Propidium Iodide Assay, Single Molecule Localization Imaging, and DNA Compaction Analysis. These diverse methodologies offer a holistic understanding of the antimicrobial efficacy and mechanisms of action of the novel rhenium-based compounds.

While rhenium has been studied for its promising anticancer effects, a comprehensive exploration of its full therapeutic potential is lacking. This thesis emphasizes the need for further research to uncover the untapped capabilities of rhenium, particularly in the context of combating antibiotic resistance.

Both the compounds show differences in results due to the fact that Re⁴⁺ is more lipophilic in nature, therefore, showing depolarization and increased membrane interactions as observed in DiSC₃(5) assay. They also show differences in DNA damage as seen in RecA localization. The findings of this study contribute insights into the development of alternative antimicrobial agents and underscore the importance of exploring unconventional metal-based complexes as

potential solutions to the escalating antibiotic resistance crisis. While one of the rhenium derivatives is fully characterized, the complete structure of the other is withheld due to its significant potential in future applications.

Furthermore, during this study a new quantification tool for image analysis of fluorescence microscopy data was utilized based on an ImageJ macro originally developed by J. Grimshaw, Newcastle University. This new method enables the quantification of nucleoid compaction from fluorescence microscopy images of bacterial cells, aiding the identification of antibiotic effects that could not be observed by eye.

Chapter 1

Introduction

1. What is Antimicrobial Resistance or Multi Drug resistance?

Antibiotics were one of history's most significant medical achievements, and their discovery changed the course of the twentieth century. Bacteria, on the other hand, quickly developed a way to survive and neutralise the effects of antibiotics. To fight the resistance challenge, increased production of new antibiotics with optimized activity and novel modes of action was adopted. However, irrational and incorrect antibiotic use has resulted in the rise of several drug-resistant bacteria, which are spreading at alarmingly high rates. New resistance traits are spreading faster than our ability to produce new antibiotics, endangering the ability to battle infectious diseases, perform surgery, and successfully transplant organs. Furthermore, pharmaceutical companies are not developing antimicrobial medications, due to the lack of funding (Chawla et al. 2022).

Antimicrobial resistance (AMR) develops when microorganisms such as bacteria, viruses, fungi, and parasites develop the ability to adapt and proliferate in the presence of drugs that previously harmed them (Dadgostar, 2019). AMR is regarded as a severe threat to public health systems worldwide, not just in developing nations. The fact that antibiotics can no longer be used to treat infectious infections foreshadows an uncertain future in health care (Salam *et al.*, 2023). AMR infection causes significant diseases such as pneumococcal infections (pneumonia, ear infections, sinus infections, and meningitis), skin infections, and tuberculosis and protracted hospitalisations, as well as increases in healthcare expenses, higher costs for second-line medications, and treatment failures. For example, in Europe alone, it is estimated that antimicrobial resistance costs more than nine billion euros each year (Salam *et al.*, 2023). Additionally, according to the Centres for Disease Control and Prevention (CDC), antibiotic

resistance adds a 20 billion dollar surplus in immediate healthcare expenses in the United States, excluding around 35 billion dollars in productivity loss per year (Dadgostar, 2019).

2. Background and Significance of Antimicrobial Resistance

Common bacterial infections, which include urinary tract infections, sepsis, sexually transmitted infections, and some forms of diarrhoea are no longer treatable by frequently used antibiotics. This happens due to the high rates of resistance indicating that we are running out of effective antimicrobial medications. In countries reporting to the Global Antimicrobial Resistance and Use Surveillance System (GLASS), for instance, the rate of resistance to ciprofloxacin, an antibiotic widely used to treat urinary tract infections, ranged from 8.4% to 92.9% for *Escherichia coli* and from 4.1% to 79.4% for *Klebsiella pneumoniae*. Common gut bacteria called *Klebsiella pneumoniae* can result in life-threatening illnesses. *K. pneumoniae* is a significant contributor to hospital-acquired illnesses include pneumonia, bloodstream infections, infections in infants, and infections among patients in intensive care units. More than half of patients treated for *K. pneumoniae* infections in some nations do not respond to carbapenem medicines due to resistance. (WHO)

Methicillin-resistant *Staphylococcus aureus* (MRSA) is a historically emerging zoonotic pathogen of public and veterinary relevance. The bacteria might infiltrate the skin, mucosal membranes, and internal organs of both animals and humans, producing significant sickness such as skin infections, acne, osteomyelitis, endocarditis, respiratory tract infection, and septicemia. Due to the release of the penicillinase enzyme, the majority of *S. aureus* strains (94%) are notably resistant to penicillin and its derivatives. MRSA is caused by strains of *Staphylococcus aureus* that are resistant to methicillin. The rise of multidrug-resistant virulent MRSA strains is a significant public health issue(Algammal et al. 2020).

MRSA is consistently resistant to a variety of antimicrobial drugs, including penicillin, methicillin, oxacillin, ceftazidime, amoxicillin-clavulanic acid, amoxicillin-sulbactam, quinolones, macrolides, cephalosporins, tetracycline, and chloramphenicol. The release of β -lactamase enzyme by *S. aureus* is the primary source of penicillin and penicillin derivative resistance, whereas the *mecA* gene (which encodes for penicillin-binding protein synthesis) is responsible for methicillin resistance. (Algammal *et al.*, 2020).

According to the WHO research, patients with MRSA infections are 64% more likely to die than those with other illnesses(Nandhini *et al.*, 2022).

3. Metal Complexes in Antibacterial Research

Antibacterial compounds are rarely "drug-like," in the sense that they do not comply to the physicochemical and reactive functionality parameters intended to guide the discovery of new orally accessible treatments. This means that many potentially innovative antibiotics have already been ruled out of synthetic libraries created with these basic drug-design axioms in mind, particularly those generated within the pharmaceutical sector (e.g., using Lipinski's Rule of Five)(Frei, Zuegg, *et al.*, 2020).

The role of antibiotic-metal complexes in modern pharmacy continues to evolve. In the face of an increasing number of drug-resistant bacteria, it is vital to seek out new, more efficient, and broadly acting antibiotics. In this regard, antibiotic-metal ion complexes have numerous options. The first review of metal ion interactions with quinolones was published over twenty years ago(Sharma *et al.*, 2022). There is currently a growing interest in the hunt for new metal ion combinations with various kinds of antibiotics and other medications. In recent years, such complexes have received a lot of attention. The primary reason for this is that many medicines have altered pharmacological and toxicological effects when they take the form of metal complexes (Ramotowska *et al.*, 2020).

3.1 Metal Complexes and their potential as Antibacterial agents

Metal ions and metal ion binding components are vital in biological processes, and their rational design could be exploited to create new therapeutic medications or diagnostic probes. Metal atoms are soluble in biological fluids due to their ability to easily shed electrons and build positively charged ions. Because they lack electrons, they can easily interact with electron-rich biomolecules like DNA or proteins, and hence contribute in either a catalytic process or the stabilization/determination of their tertiary or quaternary structures (Claudel, Schwarte, and Fromm 2020). A variety of factors, including the type of metal ion coordination complexes and organometallics, provide a diverse range of oxidation states, coordination numbers, and geometries, resulting in a virtually infinite number of structures and conformations. With improved knowledge and understanding of biological processes, strategic metal-ligand combinations with the right configuration for specific interactions can be developed. Some of them, for example, have already been used to inhibit enzymes, label proteins, image cells, probe biomacromolecules, change bioavailability, or give contrast as MRI agents (Mjos and Orvig 2014). Furthermore, the wide range of metal-ligand combinations allows for the creation of new entities with a variety of physical properties and chemical reactivities, such as charge, solubility, ligand exchange rates, metal-ligand bond strengths, Lewis acidity, metal- and ligand-based redox potentials, outer-sphere interactions, and ligand conformations (Zhang and Sadler 2017). As a result, when compared to organic medications, such complexes' structural and electrical features provide biological and chemical diversity, making them very appealing in the field of medicinal chemistry, particularly as antibacterial agents with novel modes of action to treat drug-resistant infections. In this regard, transition metals in combination with other metals appear to be the most promising for disease therapy, although heavy lanthanides are being studied for their radioactive and photoluminescent properties (Claudel, Schwarte and Fromm, 2020).

3.2 Historical context and development of Metal based Antibiotics

Since Alexander Fleming's discovery of antibiotics in the 1920s, most of the modern substances discovered by medicinal chemists around the world are almost completely organic. Although metals and their complexes have been used since time immemorial, they were mostly used as catalysts or materials, and their qualities were frequently connected with toxicity. The use of structurally defined metal complexes in medicine, on the other hand, began at the beginning of the twentieth century with the discovery of the arsenic-containing organometallic complex as the first effective treatment for syphilis (Salvarsan)(Lloyd *et al.*, 2005).

Many other metal complexes have since been discovered to be beneficial in medicinal chemistry, such as the creation of a well-known mercuric-based antiseptic agent (Mercurochrome) or the treatment of rheumatoid arthritis with a gold complex agent (Auranofin)(Gasser, 2015). However, the platinum-based anticancer medicines cisplatin, oxaliplatin, and carboplatin are unquestionably the most relevant examples in the field of medicinal chemistry(Ghosh, 2019). These complexes are still utilised as chemotherapeutic agents in about half of all cancer treatments, sometimes in combination with other medicines. Several metal-based complexes (based on silver, copper, iron gold, bismuth, gallium, etc.) have been created and tested in human clinical trials for the treatment of cancer, malaria, and neurological illnesses over the last two decades (Kenny and Marmion 2019 ; Monro *et al.* 2019).

4. Mechanism of Action

4.1 How Metal complexes exert antibacterial effect?

Despite a few, somewhat generic metal-based therapies, the inorganic chemistry area remains mostly untapped for antimicrobial uses. This is unfortunate because the enormous diversity of three-dimensional structural scaffolds made available by metal coordination chemistry is a

perfect beginning point for the study of fresh chemical space for new antibiotic compounds and provides an ideal "escape from flatland." Morrison et al's., 2022 seminal study has lately verified this argument. While the majority of organic molecules have basic one- or two-dimensional structures, the authors show that metal complexes can easily reach previously unexplored three-dimensional chemical space. (Frei, Zuegg, *et al.*, 2020).

In order to create coordination compounds, metal ions bind to organic ligands through a process known as metal complexation. Metal complexation can be utilised in antibiotic development to increase an antibiotic's activity and target range. These complexes have an antibacterial effect through a variety of mechanisms, most of which involve multiple interrelated processes (Frei, Zuegg, *et al.*, 2020).

4.1.1 Disruption of Cell Membrane Integrity :

One common way that metal-complexed antibiotic candidates work against bacteria is by rupturing the integrity of the cell membrane. The bacterial cell membrane can be targeted by metal complexes for interaction which disrupt membrane integrity (silver), leading to leakage of cellular contents and bacterial cell death. Metal complexes may generate reactive oxygen species (iron, copper), exhibit selective toxicity (vanadium) for bacterial membranes, inhibit essential functions (cobalt), and prevent biofilm formation (gallium). This can result in structural damage and increased permeability. This may cause intracellular components to leak out, which would destabilise the bacterium and eventually lead to cell death. For instance, it has been demonstrated that silver complexes damage the bacterial cell membrane, increasing the susceptibility of the bacteria to antibiotics (Frei *et al.*, 2023).

4.1.2 Reactive Oxygen Species (ROS) Generation :

The production of reactive oxygen species (ROS) inside bacterial cells is a crucial additional mechanism by which antibiotic candidates that are complexed with metals exhibit their antibacterial properties. Free radicals like superoxide and hydroxyl radicals are examples of ROS, which are extremely reactive molecules. These reactive species have the ability to seriously harm cellular constituents, which can result in the death of bacterial cells (Vatansever *et al.*, 2013).

ROS production can be induced by metal complexes interacting with bacterial cells in a number of ways. The Fenton reaction, which includes the participation of metal ions like iron and copper, is one popular method. In this process, hydrogen peroxide—a byproduct of bacterial metabolism—can be converted into hydroxyl radicals by metal complexes. Extremely harmful hydroxyl radicals have the ability to deteriorate vital biomolecules like DNA, lipids, and protein (Snezhkina *et al.*, 2020). The bacterial cells may experience oxidative stress as a result of the produced ROS, which could impair vital biological functions. Damage to DNA can impede transcription and replication, while denatured proteins can lose their ability to function. The bacterial cell membrane may become unstable due to lipid peroxidation, which would increase permeability and harm this structure. The integrity and functionality of the bacterium are compromised by the cumulative effect of ROS-induced damage (Sharifi-Rad *et al.*, 2020). Furthermore, the bacterial cell's capacity to heal the damage it has caused may be hampered by the production of ROS. Bacteria have defence mechanisms, such as catalase and superoxide dismutase, to lessen the damaging effects of reactive oxygen species (ROS). Nevertheless, these defences may be overpowered by metal-complexed antibiotic candidates, making it difficult for the bacterial cell to neutralise the excess ROS (Vatansever *et al.*, 2013).

Because of the pre-existing damage, bacterial cells are less able to respond to new stresses, which makes them more vulnerable to other antibiotics. The ultimate result of ROS generation

and the incapacity to repair the damage caused is the death of bacterial cells(Vatansever *et al.*, 2013).

4.1.3 Chelation of Essential Metals :

Chelation of key metals within bacterial cells is a significant method via which metal-complexed antibiotic candidates exercise their antibacterial effects. This mechanism can cause bacterial cell death and interfere with essential biological processes. Because essential metals like iron and zinc are involved in vital cellular functions like energy metabolism, DNA replication, and enzymatic activity, they are essential for the healthy operation of bacterial cells(Reham Z. Hamza *et al.*, 2022).

Antibiotics that have complexes with metals can sequester these necessary metals by creating stable coordination complexes within the bacterial cell. These metals' chelation prevents them from being available for use in cellular functions, which limits the bacterium's capacity to grow and survive(Reham Z. Hamza *et al.*, 2022).

Targeting bacterial pathogens, particularly antibiotic-resistant strains, can be effectively accomplished through the chelation of essential metals. Metal-complexed antibiotics effectively restrict the ability of bacteria to reproduce and sustain vital cellular functions by depriving them of the metals necessary for their growth and survival. These antibiotics therefore have a crucial function in weakening bacterial cells, increasing their susceptibility to additional antibiotics, and ultimately causing bacterial cell death (Evans and Kavanagh, 2021).

4.1.4 Inhibition of Enzymatic Activity :

The suppression of enzymatic activity within bacterial cells is a crucial method by which antibiotic candidates that are complexed with metals exhibit their antibacterial properties. This tactic is a powerful way to inhibit bacterial infections because it targets vital enzymes that are

important for many different cellular processes. These complexes contain metal ions that can interact with enzymes to disrupt their catalytic function, which in turn jeopardises the life of the bacteria (Egorov, Ulyashova and Rubtsova, 2018).

5. Effectiveness of metal complexes against MDR strains

Metal complexes have demonstrated promise in the fight against MDR strains. Many of the resistance mechanisms that these pathogens have developed can be circumvented or overcome by them thanks to their diverse mechanisms of action. Since metal complexes frequently exhibit a broad range of antibacterial activity, they are useful against both Gram-positive and Gram-negative MDR strains of bacteria. Dealing with a variety of quickly evolving MDR pathogens requires this kind of extensive activity (Baptista *et al.*, 2018). Traditional antibiotics and metal complexes can enhance each other's efficacy. This kind of synergistic effect is especially helpful in the fight against multi-drug-resistant (MDR) strains. For instance, combining metal complexes with traditional antibiotics can result in a two-pronged assault that raises the possibility of bacterial cell death. Metal complexes can lessen the effects of particular resistance mechanisms used by MDR strains by focusing on a number of vital cellular functions. It is challenging for these infections to adapt and survive because of their capacity to chelate necessary metals, interfere with enzymatic processes, and cause oxidative stress (Murugaiyan *et al.*, 2022). Cross-resistance between MDR strains and antibiotics with comparable mechanisms of action is common. Because metal complexes have different mechanisms of action, there is less chance of cross-resistance. This implies that a bacterium may still be vulnerable to metal complexes with distinct mechanisms of action even if it has developed resistance to one kind (Catalano *et al.*, 2022).

5.1 Performance Comparison to conventional Antibiotics

Comparing the efficacy of metal-complexed antibiotics versus traditional antibiotics is a crucial topic, especially when dealing with bacterial infections, especially those brought on by strains of bacteria that are resistant to multiple drugs (MDR). Aspects of their performance that are evaluated in this review include safety, resistance mechanisms, efficacy, and potential application (Sánchez-López *et al.*, 2020).

5.1.2 Resistance Mechanisms :

Further investigation into the mechanisms underlying decreased cross-resistance is imperative (Davies, 1996). Antibiotics that are complexed with metals can counteract certain resistance mechanisms that bacteria use. Their capacity to target metalloenzymes, like β -lactamases, which are crucial in the development of antibiotic resistance, is a prime example. Metal complexes can increase the potency of traditional antibiotics by blocking these enzymes. To comprehend how metal complexes interact with resistance mechanisms, it is essential to look into the precise pathways through which they do so (Kotränge *et al.*, 2021).

5.1.3 Safety :

Sometimes, particularly when taken in large doses, conventional antibiotics can have harmful side effects and be toxic. If the metal and ligand selection is done carefully, metal-complexed antibiotics may be used in a safer manner. Comprehensive toxicological studies are necessary to assess the possible risks associated with particular metal complexes and ligands in order to gain a deeper understanding of the safety profile (Evans and Kavanagh, 2021).

Chapter 2

Scope of the study

This section will provide the outline of the project and describe the theoretical background and topics included in this research, focusing on the antibiotics and experimental methods used.

1. Rationale of the Thesis

The experiment involves tests and assays on two rhenium derivatives to check their modes of action and function on *Bacillus subtilis* 168CA cells. The two derivatives were used in order to draw a comparison study and collect data to determine how both behave under certain conditions and if they exhibit bactericidal properties when used in different concentrations. Re4 has an additional Phenyl-unit in its R-groups, therefore most likely is more lipophilic and slightly larger in size. The true structure of Re4 could not be stated due to its potential and unpublished studies.

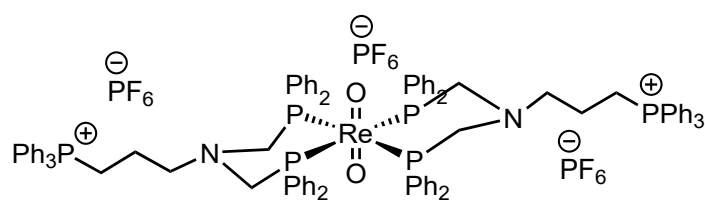


Figure 1. Structure of Re1

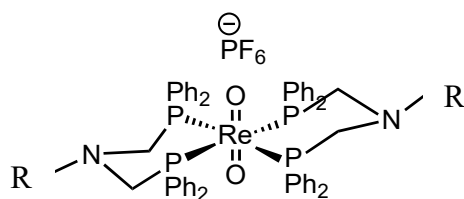


Figure 2. Structure of Re4

1.1 Why Rhenium Complex?

Recently, metallodrugs based on rhenium have been emphasised as potentially effective options for novel antibiotics against bacteria that are resistant to drugs (MDR). Many transition metal complexes, including those formed from ruthenium, have been investigated as possible antibiotics within the past ten years. Even though rhenium compounds are currently of great interest for anti-cancer applications, they have not received as much research (Cooper *et al.*, 2022).

Despite being among the top ten most costly metals, it is still less expensive than platinum, which is frequently used in cancer treatments. Its peculiar valence electrons arrangement permits a large variety of oxidation state supporting a diverse set of ligand types and coordination geometries. It is possible to modify the ligands' lipophilicity, luminescence, cellular uptake, biodistribution, cytotoxicity, and pharmacological and toxicological profiles by fine-tuning them in the metal environment (Collery, Desmaele and Vijaykumar, 2019).

For ReI, previous studies suggest that nanomolar concentrations of it have been shown to be effective against Gram-positive pathogens, including methicillin-resistant *S. aureus* (MRSA) and *Enterococcus faecium*. Although some of the most powerful complexes exhibit strong interactions with DNA, suggesting that DNA may be a potential target for their mode of action, the molecules have no effect on the potential of bacterial cell membranes. Even at significantly higher doses of the corresponding MICs, the complexes with anti-staphylococcal/MRSA activity were not harmful to the organism, according to *in vivo* studies conducted in the zebrafish model (Sovari *et al.*, 2020).

1.2 Antibiotics

This work is a component of a larger investigation into the *in vivo* processes of clinically important antibiotic classes being conducted at the Wenzel lab at Chalmers University of Technology's Division of Chemical Biology. The most relevant structural and mechanistic types of antibiotics, which are further classified into those that target the cell envelope and those that have intracellular targets, are studied in this project. Apart from performing experiments using Re1 and Re4 simultaneously, other antibiotics were used as positive controls in this study as described in table 1. In this thesis, their effects on DNA and the cell membrane are investigated to obtain an overview of all possible targets and downstream effects. While more detailed analyses would be possible, the scope of the thesis was the generation of a broad overview of Rhenium compounds as potential antimicrobial candidates.

Table 1. Antibiotics used in this study, their known target and their intracellular mechanism of action in bacterial cells

Antibiotics	Target	Intracellular mechanism
Ciprofloxacin	Bacterial DNA gyrase and topoisomerase IV, which are enzymes involved in DNA replication, repair, and recombination.	Inhibits the activity of DNA gyrase and topoisomerase IV, leading to DNA strand breaks, disrupted DNA replication, and ultimately, bacterial cell death.
Gramicidin	Forms ion channels in bacterial cell membranes,	They allow the passage of ions across the bacterial cell membrane, leading to a loss of ion balance and eventual cell lysis

	leading to membrane disruption and cell death	
Vancomycin	Vancomycin targets the bacterial cell wall by binding to the D-Ala-D-Ala terminus of peptidoglycan precursors	Vancomycin weakens the bacterial cell wall, causing it to rupture and leading to cell death.
Mitomycin C	It targets DNA by forming cross-links between DNA strands, preventing DNA replication and transcription.	Mitomycin forms interstrand cross-links in the DNA molecule, inhibiting DNA replication and transcription.
Nisin	Nisin primarily targets the cell membrane of bacteria, especially Gram-positive bacteria.	Nisin interacts with a precursor molecule called Lipid II, which is involved in bacterial cell wall synthesis.

1.3 Experimental Assays:

In order to understand how to optimise the use of currently available antibiotics and to provide critical information for the development of new antimicrobial agents, it is imperative that we investigate the antimicrobial mechanism of lesser-known antibiotics and how those impact the intracellular pathways and cellular processes in living bacteria cells. The model organism in

this study was *Bacillus subtilis* 168CA, one of the best-characterized Gram-positive model bacteria. It shares close kinship with numerous significant pathogens, such as *Listeria monocytogenes*, *Staphylococcus aureus*, *Clostridium difficile*, and *Streptococcus pneumoniae* (Pedreira, Elfmann and Stülke, 2022). *B. subtilis* is a safe substitute model organism because it is regarded as a GRAS (Generally Regarded As Safe) organism in and of itself. Being one of the most thoroughly studied gram-positive bacteria, it also offers a wealth of background knowledge on things like protein-protein interactions, expression patterns, metabolic pathways, and regulatory components. Moreover, *B. subtilis* grows quickly and is simple to sub-culture (Pedreira, Elfmann and Stülke, 2022).

Previous studies in this lab suggest that the Rhenium compound might possess a secondary mechanism of action. In this study, we specifically looked for a concentration that would be more or less inhibiting than in the previous project. These new concentrations will allow us to determine if the previously observed effects are concentration dependent.

This study focused on the effect of Rhenium compounds on one generation of *B. subtilis* cells. Since this bacterium has a doubling time of approximately 20-30 minutes at 37°C, effects after 30 minutes of treatment were investigated (Errington and van der Aa, 2020)

The fluorescence microscopy technique is a non-invasive and established method to visualize living bacterial cells. In this study, bacterial cytological profiling (BCP) was included to gain insight into how antibiotics affect cell morphology. This technique has been aiding various mode of action studies by combining a membrane dye, a DNA dye, protein fusion, and phase contrast microscopy (Nonejuie et al., 2013, Wenzel et al., 2018).

Protein localization studies using reporter gene fusions were performed to explore which intracellular proteins were affected by antibiotic treatment. The utilization of these assays provided direct visualization of the protein localization within the cell (Schäfer and Wenzel, 2020) .

The Rhenium compounds used in this study must cross the membrane to reach intracellular targets. Therefore, this study also looked at changes in different membrane properties in relation to antibiotic treatment. More specifically, the depolarization effect of antibiotics was investigated, by utilizing the membrane potential DiSC₃(5). In addition, during this study, a quantification tool for image analysis of fluorescence microscopy data was utilized based on an ImageJ macro originally developed by J. Grimshaw, Newcastle University. This new method enables the quantification of nucleoid compaction from fluorescence microscopy images of bacterial cells, aiding the identification of antibiotic effects that could not be observed by eye.

Chapter 3

Materials and Methods

1. Minimal Inhibitory Concentration

The lowest concentration of an antibiotic that will stop a microorganism from growing visibly after an overnight incubation is known as a minimum inhibitory concentration (MIC), and the lowest concentration of an antibiotic that will stop an organism from growing after it has been sub-cultured onto media free of antibiotics is known as a minimum bactericidal concentration (MBC). Diagnostic labs use minimum inhibitory concentrations (MICs) primarily to confirm antibiotic resistance, but they are also frequently used as a research tool to assess new antimicrobials' in vitro activity(Andrews, 2001).

Preparation

Bacterial cultures were grown in Luria-Bertani (LB) medium, the components for the medium are shown in table below. The LB medium was autoclaved to ensure sterility.

Table 2. Components in LB media

Material	Amount
NaCl	10 g
Tryptone	10 g
Yeast extract	5 g
MilliQ-water	1 L

Prepared a 50% glycerol stock for long-term storage of bacterial samples. A 50% glycerol solution was prepared by diluting 100% glycerol in dH₂O.

A lower MIC value indicates that less of the drug is required in order to inhibit growth of the organism, drugs with lower MIC scores are more effective antimicrobial agents. For this the *168CA* cells were grown overnight as described above and diluted. A 96-well plate was prepared as given below.

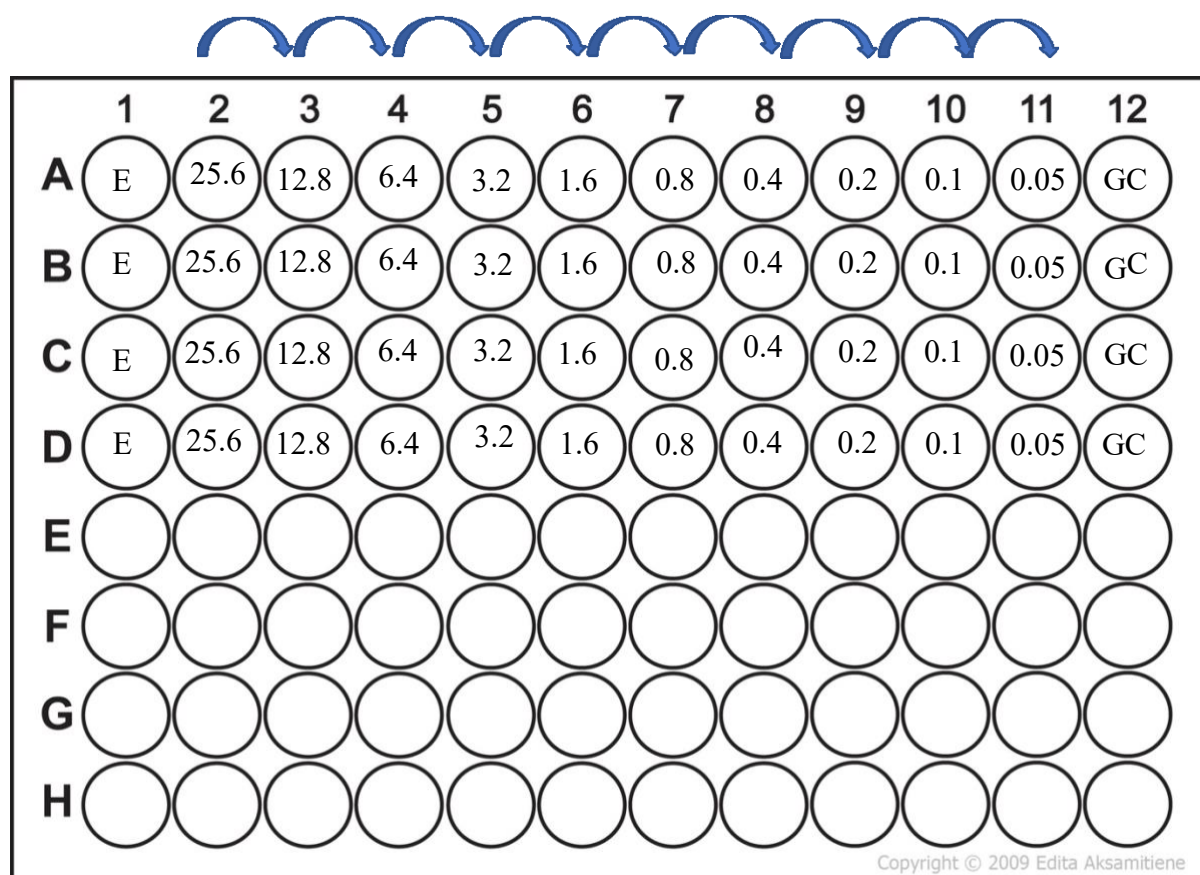


Figure 3. 96-well microtiter plate preparation for the determination of Minimal inhibitory concentration. The E in the microtiter plate denotes sterile control and GC is the growth control. The values are in μM and denotes the reducing concentration of compounds.

200 μl of LB was put in E and the next well. 100 μl of LB was put from the 3rd well until 11th well. Before the next step a solution was prepared of both the Rhenium compounds and DMSO. Filtered DMSO was used for this purpose. Rhenium compounds were added in a ratio of 1:100 i.e., 2 μl of Re compounds were added to 198 μl of DMSO. After addition of compounds Performed serial dilution upto 11th well. 100 μl of the bacteria at OD600 = 0.3 was added to the plate from 2nd well till the 12th i.e, the growth control.

The plate was sealed with parafilm and kept in the incubator at 37° C overnight.

2. Growth curve

By monitoring the optical density, the growth curve describes how bacteria multiply over time in a liquid culture. Lag phase (non-replicative period), exponential phase (replicative period), stationary phase (cell growth arrest period), and decline phase (cell death period) are the four distinct growth phases that can be identified (Bertranda, 2019).

Growth curve studies were performed to investigate both antibiotic's optimal stressor concentration (OSC) when added to exponentially growing cultures, that results in growth inhibition of *B. subtilis*. A reduction of the growth rate of 50-70% was aimed for, depending on the individual antibiotic.

Bacillus subtilis 168CA was inoculated in 2 ml sterile LB medium under sterile conditions. The culture was grown overnight at 37°C with continuous shaking. The culture was diluted in the morning as stated above and grown until OD₆₀₀ = 0.3.

A 96-well plate was taken and four concentration of Re compound were added in the plate as shown below:

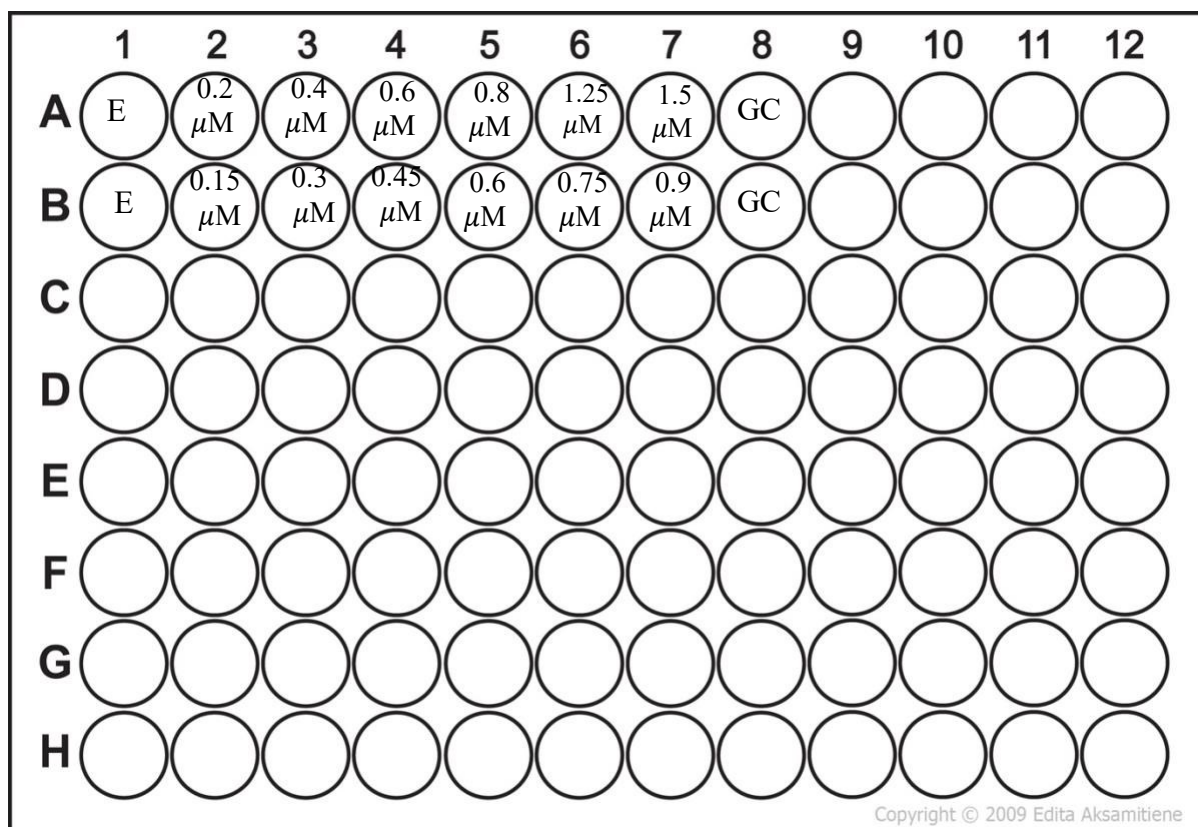


Figure 4. 96-well microtiter plate assembly to determine the growth curve using absorbance spectrophotometry where row A contains Re1 whereas row B contains Re4. The E in the microtiter plate denotes sterile control and GC is the growth control.

200 μl of 168CA culture at $\text{OD}_{600} = 0.3$ were added from wells 2 to 6. 200 μl of sterile LB was added in the 1st well. The Re compounds were diluted 2 μL in 198 μL of DMSO and was added in the plate as given above.

To perform the growth curve assay the CLARIOstar^{PLUS} platereader from BMG LABTECH was used. The plate was placed in the microplate reader when the incubator in the plate reader showed 37° C temperature. The absorbance at OD_{600} was measured for 16 hours until the cells reached the stationary phase. Three biological replicates were made for the same assay.

3. DiSC₃(5) diffusion assay

Consequently, a different assay is required to measure the membrane potential, such as the voltage-sensitive dye DiSC₃(5) (Schäfer and Wenzel, 2020). DiSC₃(5) is a cationic membrane-permeable fluorescence dye with self-quenching properties. It accumulates in polarized cells and is released upon depolarization leading to an increased fluorescence signal (te Winkel *et al.*, 2016) (Fig 4). These properties of DiSC₃(5) enable it to detect membrane depolarization triggered by antibiotics. Here, it is necessary to verify that the antibiotics compounds of interest do not alter the fluorescence reading significantly. This is covered by performing the assay in the absence of cells as an additional control (te Winkel *et al.*, 2016)

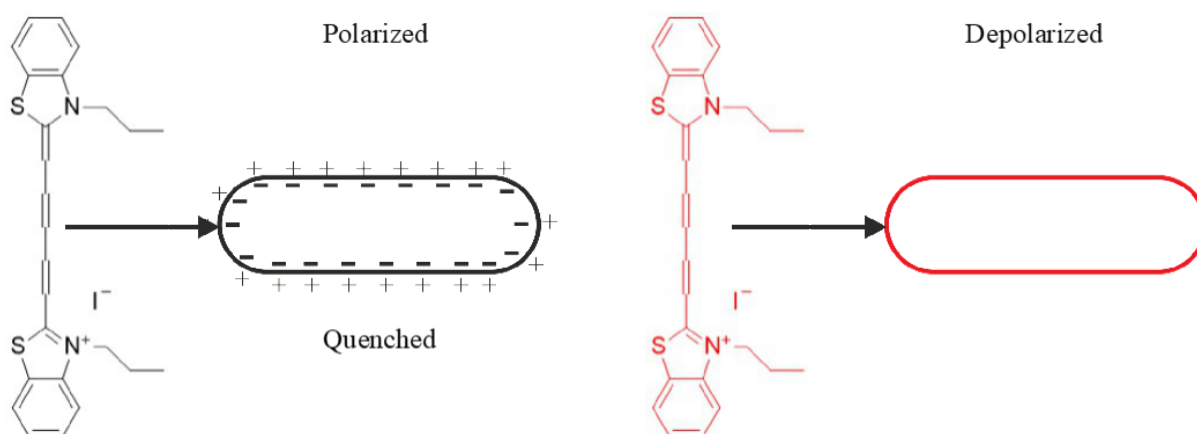


Figure 5. Membrane depolarization assay with DiSC₃(5). The dye accumulates at the polarized membrane and is released when the cell depolarizes. The release of the dye results in an increased fluorescence signal (Schäfer and Wenzel, 2020).

The effect of antibiotics on the membrane potential was assessed using the DiSC₃(5) assay. The probe of DiSC₃(5) accumulates on the hyperpolarized membrane and is released once the membrane gets depolarized, which leads to an increase in fluorescent signal in spectroscopic assays (te Winkel *et al.*, 2016).

The *B. subtilis* 168CA was inoculated to sterile 2 mL LB containing 50 mg/mL BSA in a 50 mL falcon tube and incubated overnight at 37°C under continuous shaking. The overnight culture was then diluted in 2 mL LB containing 50 mg/ml BSA.

Once an OD₆₀₀ of 0.3 was obtained, 138.5 ml of the diluted cells containing BSA were transferred to a COSTAR 96 microtiter plate. Medium containing BSA was also transferred to separate wells. The kinetic assays using DiSC₃(5) were done using the CLARIOstar^{PLUS} platereader from BMG LABTECH.

To perform the DiSC₃(5) assay mixed 20 ml of LB with 100 µl of BSA. 85 µl of this solution was mixed with 15 µl of DiSC. After the incubator temperature reaches 37° C, 138.5 µl of diluted cells (in medium + BSA) transferred to a microtiter plate in 6 wells and 138.5 µl of LB+BSA in 7th well (no cells). The plate setup can be seen below.

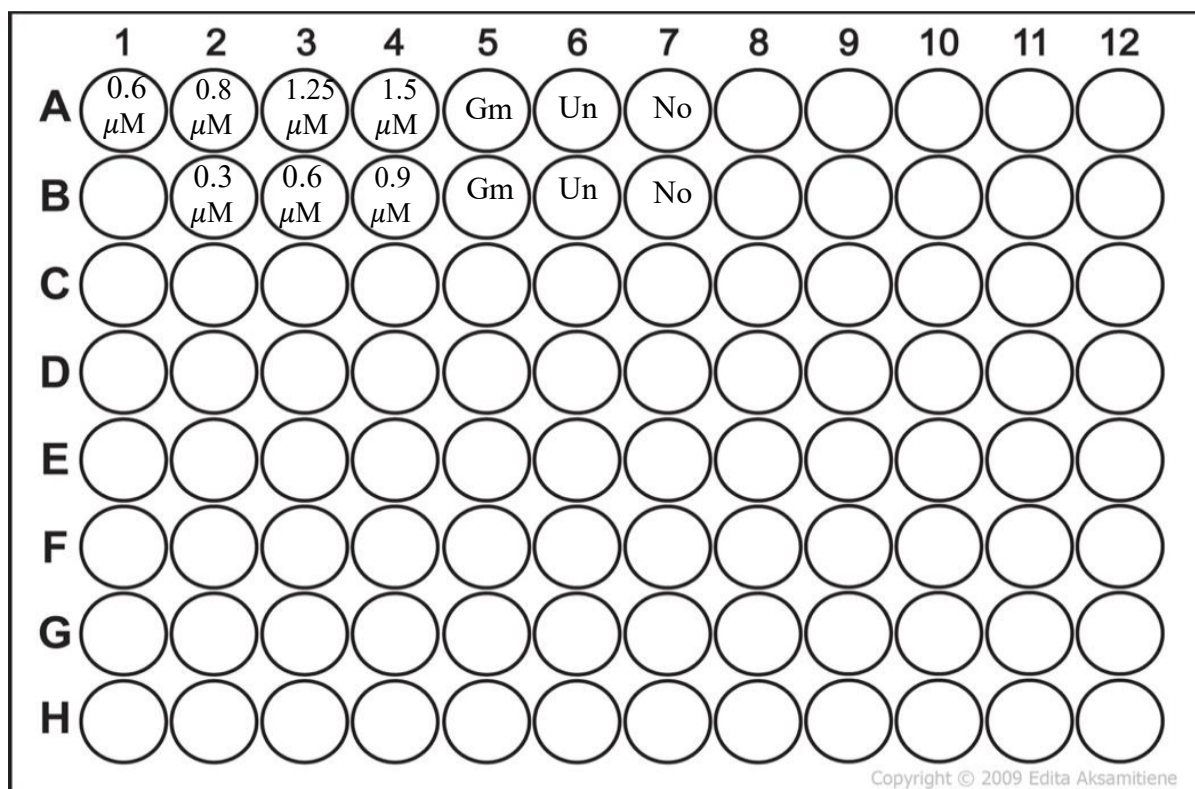


Figure 6. 96-well plate assembly for the measurement of fluorescence with DiSC₃(5) where Row A represents concentrations of Re1 and Row B represents concentration of Re4 used to treat cells. Gm represents Gramicidin used as a positive control. The 6th well denotes untreated cells and the 7th well contains only compounds and medium.

Started the assay (we measure every 20 sec) and recorded baseline without DiSC and with only the cells and media in 7 wells. After the graph reaches a baseline, 10 μ l of 15 μ M DisC3(5) was added in all the 7 wells. Restarted the run for the fluorescence level of the ‘no cells’ control to reach a stable signal, at this time the fluorescence level in the wells containing cells should also have reached a stable level (this happens very rapidly, <1 min). Paused the run.

The first 4 wells were where different concentration of Re compound was added. To calculate the volume of compound we use :

$C1V1 = C2V2$, this time for a total of 150 μ l of samples (138.5 μ l of cells/media + 10 μ l of DisC3(5) + compounds)

Therefore,

Added 1.5 μ l of 100 μ g/ml Gramicidin in the 5th well. The 6th well denotes untreated cells and 7th well has no cells. Restarted the run as long as needed until reached baseline.

4. Bacterial cytological profiling (BCP)

Bacterial cytological profiling (BCP) is a method that was originally developed by (Nonejuie *et al.*, 2013). Within the context of mechanism of action studies, BCP is a potent, quick, and one-step method used to explore the cellular route that antibiotic compounds target. This technique enables the simultaneous phenotypic analysis of two or more cellular parameters by combining different fluorescence dyes. A membrane dye (NileRed), a DNA stain (DAPI), and a strain of *B. subtilis* that expresses cytosolic GFP (PrpsD-GFP) were used in this investigation. This combination makes it possible to monitor membrane damage (shown by an irregular membrane stain), DNA packing defects (shown by a condensed or dispersed nucleoid stain), and pore formation (shown by GFP leakage or decrease in signal) all at the same time. Additionally, the phase contrast channel is included to provide information on cell morphology.

To quantify antibiotic effects on nucleoid compaction, an ImageJ macro originally developed by James Grimshaw, Newcastle University, was used. This macro analyses cells by using the ratios of the whole cell area (based on phase contrast) and the fluorescent nucleoid area, thereby calculating nucleoid compaction. The phase contrast channel is additionally included to offer details on cell morphology. Using image analysis, the effects of antibiotic treatment were quantified in terms of membrane changes, variations in DNA compaction.

The *Bacillus subtilis* strain MW54 (PrpsD-GFP) expressing cytosolic GFP was used for the bacterial cytological profiling. MW54 was inoculated in 2 mL sterile LB and incubated overnight at 37°C under continuous shaking. The overnight culture was diluted and grown until an OD₆₀₀ of 0.3 was reached. Subsequently, 100 µl of overnight culture was distributed to four pre-warmed 2 mL Eppendorf tubes, which were kept on a thermomixer at 37°C with 750 rpm. The Re compounds were added and incubated for 30 minutes. The concentration of Re compound added were:

For 100 µl of culture the same concentration was calculated as above.

Therefore, 1.2 µl, 1.6 µl and 2.5 µl of Re1 compound was added for treatment in 3 eppendorf tubes. For Re4, 0.6 µl, 1.2 µl and 1.8 µl of the compound was added. 1 tube was left Untreated for both compounds to check the comparison between treated and untreated cells.

12-well microscopy slides were prepared using 800 µl of 1.2% agarose. The DNA stain DAPI (1 µg/ml) and membrane stain NileRed (0.5 µg/ml) were added to each sample at 25th minute of treatment for 5 minutes. Here, *B. Subtilis* already expresses cytosolic GFP used to check membrane damage by pore formation by GFP leakage.

0.5 µl of each sample was pipetted on the microscopy slides for observation and covered with dopamine coverslips. The adhesive and biocompatible nature of dopamine-coated slides make

them suitable for cell culture studies. Cells can adhere and grow effectively on these surfaces. 3 biological replicates were made for the same.

The image was observed using fluorescence microscope and the images were analysed by using ImageJ: James Grimshaws Macro (Newcastle University) and MicrobeJ was used to quantify the nucleoid compaction from the DAPI channel.

For compaction analysis, The principle by which the macro analyses a cell is by calculating the nucleoid compaction utilizing the ratio of cell area and nucleoid area. In this method, bacterial cells are selected manually by selecting a region of interest (ROI) with four polygonal boundaries. The macro is run in ImageJ/Fiji and the data obtained is used to compare the samples and deduce the effect observed in the treated and untreated samples.

5. Protein localization study

Fluorescent protein fusions to various cellular proteins have been used in protein localization assays in living cells. The functions of the proteins within the cell dictate the patterns and ways in which they localise. Crucially, some antibiotic therapies have the ability to delocalize these useful proteins, which renders them inactive. As a result, target identification and antibiotic mode of action diagnosis are possible with protein localization assays (Saeloh *et al.*, 2018).

In this study, GFP fusions to proteins involved in different intracellular processes were used, including DNA damage repair (RecA), DNA replication (DnaN), cell shape determination, chromosome segregation (MreB) etc.

In order to investigate the impact of Re compounds on different intracellular processes, various GFP-tagged reporter proteins expressed by genetically recombinant *B. subtilis* were used. The strains used in this study and their genotype are displayed in table 3.

Strains were inoculated in 2 mL sterile LB. Strains that required induction for promoting the expression of the GFP-tagged proteins were supplemented with xylose (table 3). All cultures were incubated overnight at 37°C with continuous shaking. On the following morning, the overnight cultures were diluted in 2 mL sterile LB along with the required xylose concentration and grown to an OD₆₀₀ of 0.3.

100 µl of culture was transferred to 2 mL Eppendorf tubes and treated with Re antibiotics at 37°C and 750 rpm for 30 minutes. 12-well microscopy slides were prepared using 800 µl of 1.2% agarose. Once the 30 minutes incubation was completed, 0.5 µl of each sample was placed on the microscopy slide. Each experiment was replicated three times. Image analysis was done with ImageJ software and was adapted to each strain's analysis

Table 3. B. subtilis and genotypes used for protein localization assay and inducer concentrations used for each strain

Protein	Strain	Genotype	Inducer
DnaN	HM771	gfp-dnaN::cat	-
RecA	UG10	amyE::Pxyl_recA-mgfp spc	0.5% xylose
MinD	TB35	amyE::spc Pxyl-gfp-minD	1% xylose
MreB	KS69	amyE::spc Pxyl-msfgfp-mreB	1% xylose
YocM	MS44	Pxyl-yocM-gfp	0.5% Xylose

6. Single Molecule Localization Imaging

Single molecule localization imaging is an advanced microscopy technique that is used in the field of biological imaging, enabling visualization and study of molecular processes at unprecedented resolutions. When applied to the investigation of DNA damage and repair, this technique provides a powerful tool for understanding the dynamics of these crucial cellular events at the single-molecule level (Martens *et al.*, 2022).

Single molecule localization imaging can be employed to visualize DNA lesions. Specific fluorophores can be attached to DNA repair proteins or markers, allowing researchers to track and visualize individual repair events. By tracking individual repair events, researchers can quantify the efficiency of DNA repair processes. This can be particularly valuable for understanding variations in repair rates under different conditions or in the presence of specific DNA damage-inducing agents. Single molecule localization imaging enables the dynamic tracking of molecular events over time, providing a more comprehensive understanding of the temporal aspects of DNA damage and repair (Zalejski, Sun and Sharma, 2023).

To investigate DNA damage and repair by fluorophores attached to DNA repair markers.

Table 4. Enzymes used and their functions

Enzymes	Functions
APE1	Repairs apurinic/apyrimidinic (AP)-sites. Recognizes and removes uracil, alkylated and oxidized bases and AP-sites.
<i>Fpg</i>	Recognizes and removes various types of oxidized purines, for example 8-oxoguanine
<i>Endo iii</i>	Can remove oxidized pyrimidines
<i>Endo iv</i>	Apurinic/apyrimidinic (AP) endonuclease, repairs oxidative DNA damage

<i>Endo viii</i>	Repairs various types of damaged pyrimidines, including oxidized pyrimidines
<i>UDG</i>	Catalyzes the removal of uracil from DNA, such as those caused by deamination of cytosine to uracil

Briefly, an enzyme master mix (Table 5) was prepared in 1X CutSmart Buffer, 100 ng DNA and milli-Q water to a total volume of 50 μ L per sample. Alternatively, single enzymes were added to 100 ng DNA, 1X CutSmart Buffer, and milli-Q water. The mixture was incubated (37°C) for 1 hour. A nucleotide master mix (Table 6) was prepared in 1.25 U DNA polymerase 1, 1X NEBuffer 2 and milli-Q water to a total volume 100 μ L per sample. It was incubated (20°C) for 1 hour before the addition of 0.25 M Ethylenediaminetetraacetic acid (EDTA) to stop the ongoing reaction. During and after addition of the fluorescently labeled nucleotides, the experiments were performed in minimum light exposure. The samples were stored in -20°C wrapped in aluminium foil.

Table 5. The enzymes used for DNA damage labelling and the corresponding concentrations

Enzymes	Concentration (U)
Ape1	2.5
Endo III	2.5
Endo IV	2.5
Endo VIII	2.5

Fpg	2.5
UDG	2.5

Table 6. The nucleotides used for DNA damage labelling and the corresponding concentrations

Nucleotide	Concentration (uM)
dATP	1
dCTP	1
dGTP	1
dTTP	0.25
Aminoallyl-dUTP-ATTO-647 N	0.25

For staining and imaging, typically 7 μL of fluorescently labelled DNA was diluted in 0.5X Tris-borate EDTA (TBE) and stained with 320 nM YOYO-1. In addition, 1 μL β -mercaptoethanol was added just before the image acquisition to reduce photobleaching. From the final volume of 50 μL , 3.2 μL was placed at the interface of a functionalized coverslip and a microscope glass slide. A drop of immersion oil was put on the coverslip and the imaging was performed with a 100X objective on a Zeiss Observer Z1 fluorescence microscope with a Photometrics Prime 95B sCMOS 22mm camera. Two channels were used for imaging, YOYO-1 (emission wavelength 508 nm) and ATTO-647 (emission wavelength 679 nm). The light source intensity was set to 8% and 31.1% the exposure times were set to 500 ms and 1200 ms for YOYO-1 and ATTO-647, respectively.

Before imaging, the coverslips had to be functionalized to allow stretching of the DNA. Coverslips (22x22 mm) were arranged in a rack and immersed in a mixture of 1% v/v of 3-Aminopropyltriethoxysilane (APTES) and Allyltrimethoxysilane (ATMS) in acetone for at least 2 hours. Prior to use, they were rinsed in a solution containing acetone and milli-Q water (2:1) and dried with nitrogen gas.

Chapter 4

Results and Discussions

1. Minimal Inhibitory Concentration

The optimal stressor concentration (OSC) values were determined by comparing the growth inhibition of the treated sample to the untreated control. The MIC that inhibited the visible growth of *B. subtilis* 168CA after overnight incubation were 0.4 μM for Re1 and 0.3 μM for Re4. The values were confirmed by creating technical replicates.

Previous studies state that in 2017 Siegmund et al., described the preparation of novel Re(I) *N*-heterocyclic carbene (NHC) complexes. These compounds were found to possess potent antibacterial activity against Gram(+) strains, while being inactive against Gram(-) ones (MIC_{*B. subtilis*} = 0.7–1.3 μM , MIC_{*S. aureus*} = 0.7 μM). The authors introduced later a series of *N*-heterocyclic carbene diimine complexes of the metal ion showing high activity against Gram-positive strains, including MRSA, with MIC values of 0.7-2 μM (Siegmund *et al.*, 2017). Frei and co-workers presented the antibacterial activity of rhenium bisquinoline species, which can be photo-activated against drug-resistant *S. aureus* and *E. coli* with similarly low MIC values (Frei, Amado, *et al.*, 2020). These studies contribute and help us determine the activity of different Rhenium derivatives.

2. Growth Curve

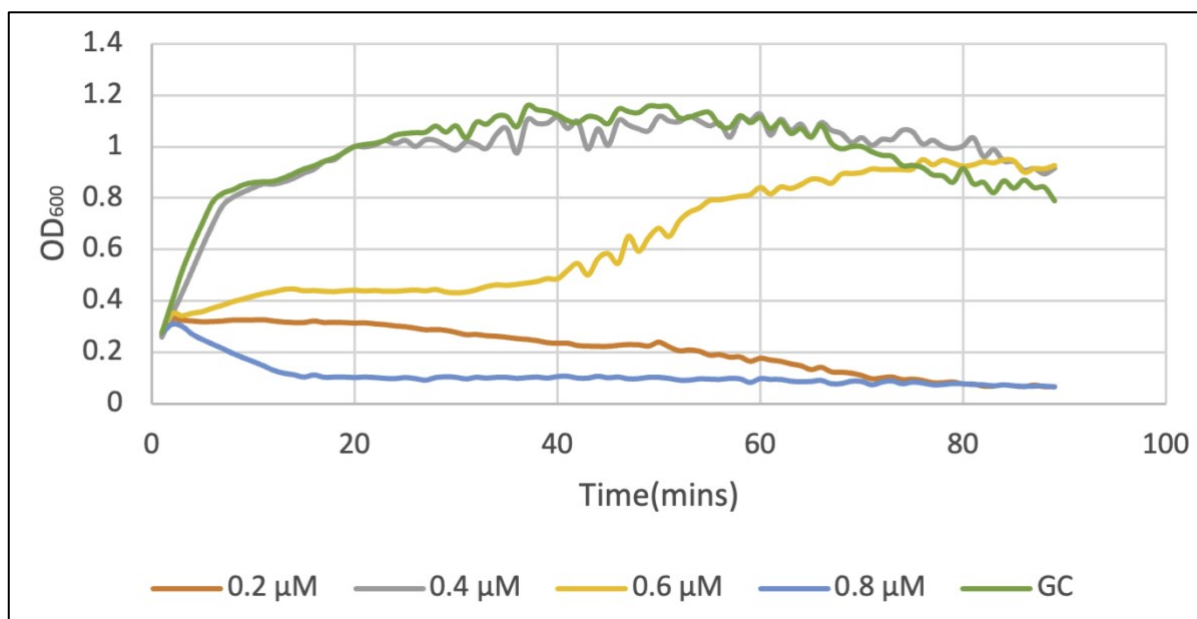


Figure 7. Growth Curve for Re1 with different concentration of Re1 added to cells. GC denotes the growth control which does not contain Re1 compound

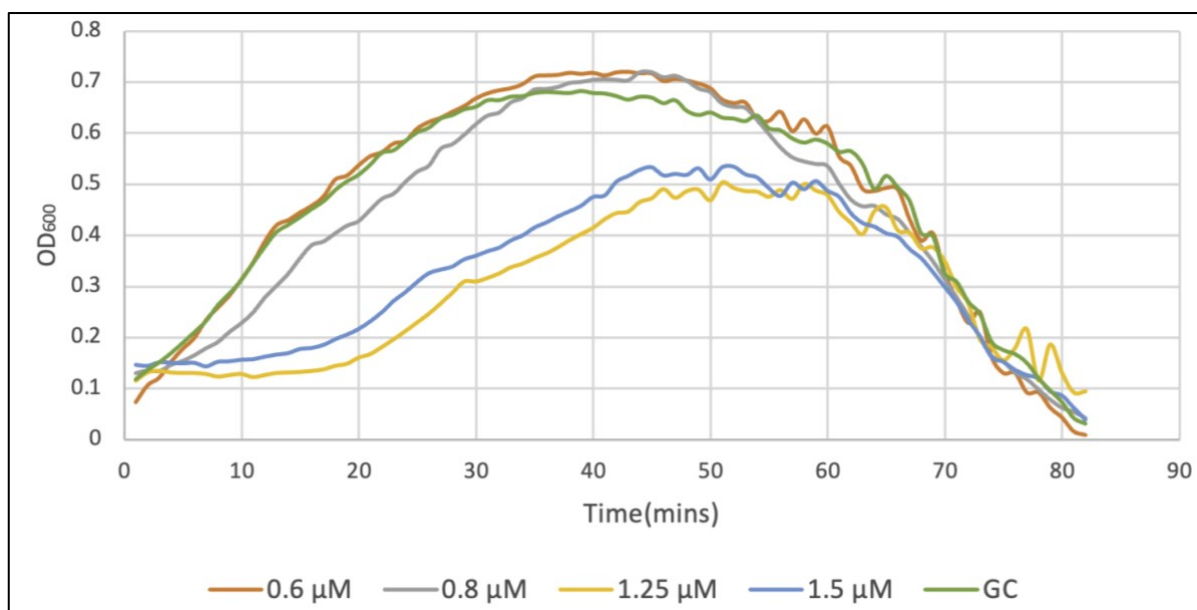


Figure 8. Growth Curve for Re1 with different concentration of Re1 added to the cells. GC denotes the growth control which does not contain Re1 compound

The above graphs represents growth curve for Re1 compound which was done in two rounds to check its effects in gradually rising concentrations. Both the growth curves were performed

with gradually increasing concentrations. The graphs, however, show different curves for the common concentrations. This could be due to an uneven distribution in solution or instability. After the preparation of technical replicates, three concentrations were chosen to perform microscopy assays and check various other cellular parameters. 0.6 μM , 0.8 μM and 1.25 μM concentration were chosen to check the membrane damage, pore formations and various other cellular route that antibiotic compounds target.

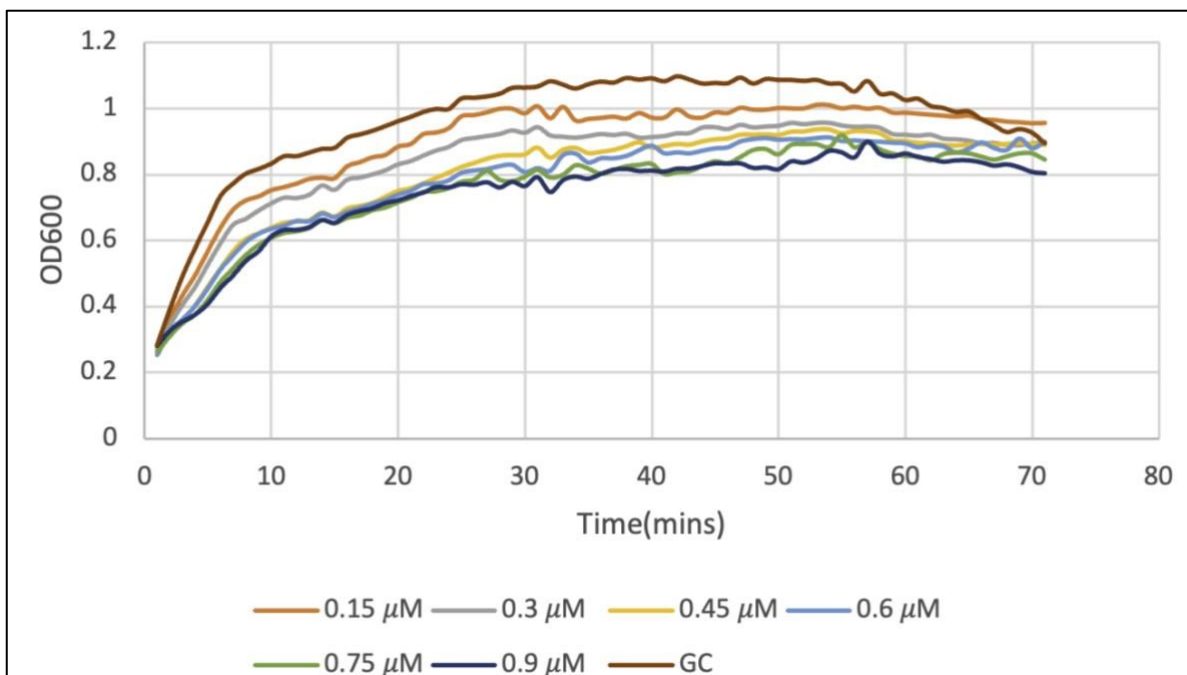


Figure 9. Growth Curve for Re4 with different concentration of Re4 added to the cells. GC denotes the growth control which does not contain Re4 compound

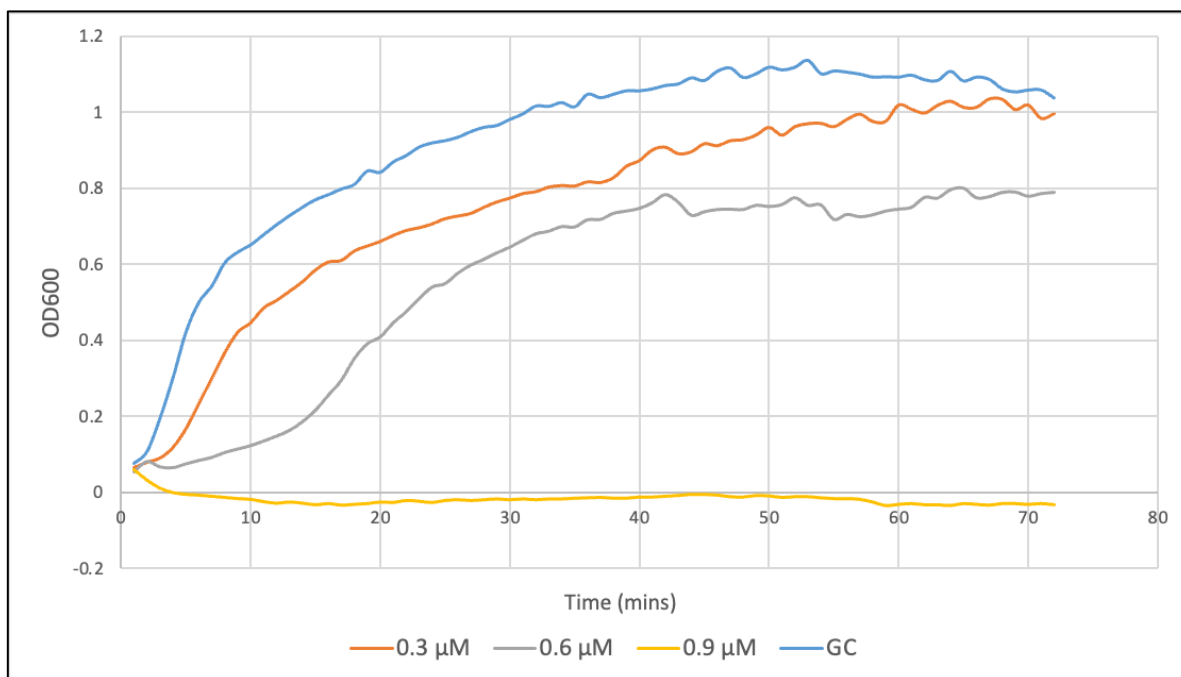


Figure 10. Growth Curve for Re4 with different concentrations of Re4 added to the cells. GC denotes the growth control and does not contain Re4 compound

The above graphs represents growth curve for Re4 compound which was done in two rounds to check its effects in gradually rising concentrations. Both the growth curves were performed

with gradually increasing concentrations. The graphs, however, show different curves for the common concentrations. This could be due to an uneven distribution in solution or instability. After assessing the technical replicates, the concentrations chosen for further tests were 0.15 μM , 0.3 μM and 0.45 μM .

3. DISC₃(5) Diffusion Assay

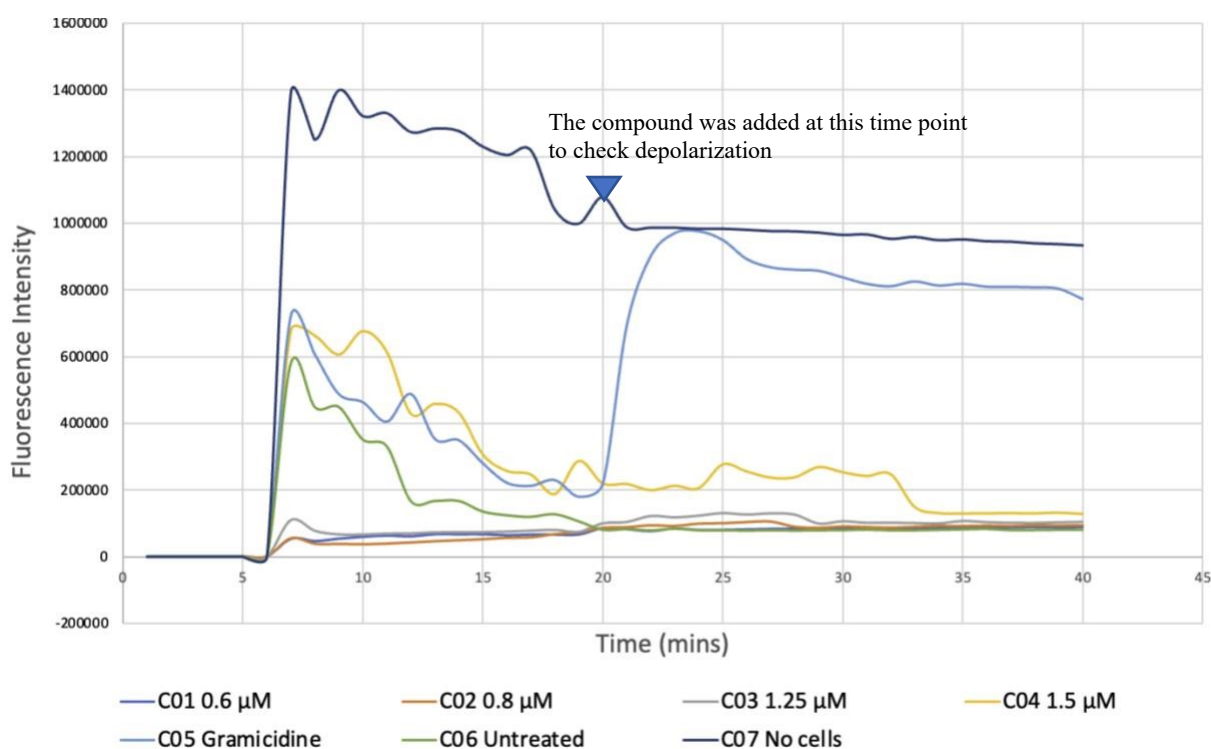


Figure 11. DiSC₃(5) Diffusion Assay for Re1

The above curve shows that there is no depolarization occurring when treated with Re1 compound since there is no increase in fluorescent signals after treatment with DiSC stating that the depolarization is not occurring in this case. It was further confirmed by the technical replicates.

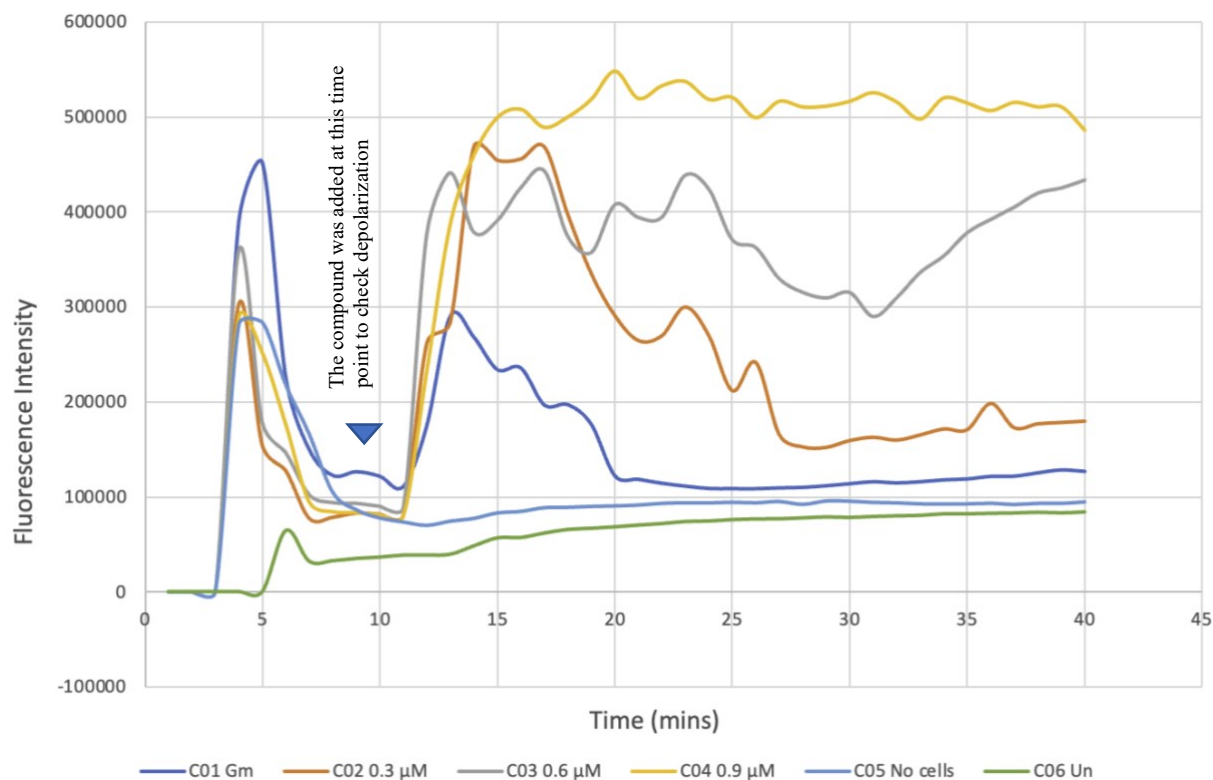


Figure 12. DiSC₃(5) Diffusion Assay for Re4

On the other hand, for Re4 compound, there is a spike in signal when DiSC₃(5) was added which clearly suggests that depolarization is taking place in this case. It was further confirmed by preparing technical replicates which gave similar results. By being more lipophilic it increased membrane interaction, which might have favoured the depolarization.

4. Bacterial Cytological Profiling

The results of the bacterial cytological profiling assay can be observed in figure 13 for Re1. The cytosolic content, based on the GFP images, of all tested conditions, was bright green and visible in the whole cytosol of the cells. This indicates that no cytosolic leakage occurred. Furthermore, no signs of cell lysis or other morphological changes were observed in the phase contrast images.

In untreated control cells, the DAPI stains showed a regular pattern with evenly sized and regularly distributed nucleoids, which indicates normal nucleoid packing and distribution in the cells.

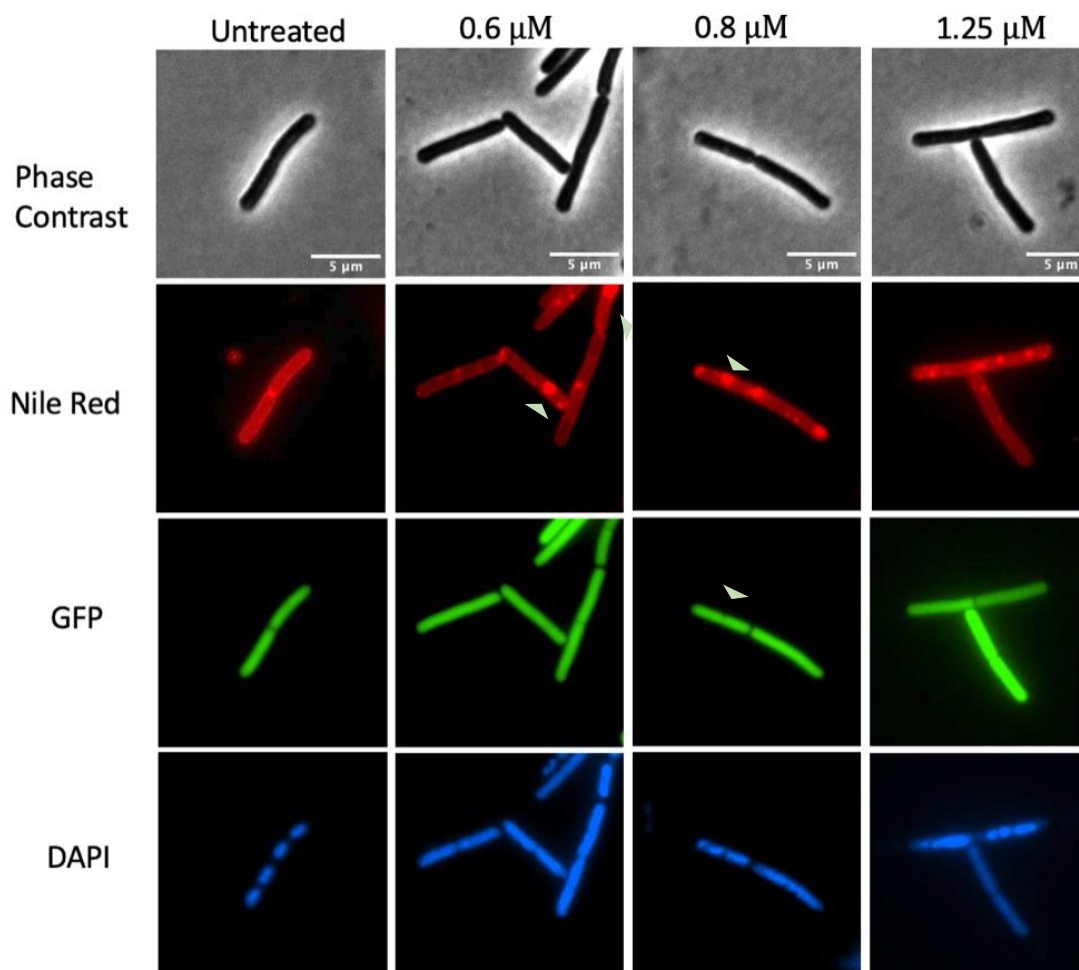


Figure 13. Bacterial Cytological Profiling of MW54 cells using Re1 with Nile red, GFP and DAPI stains

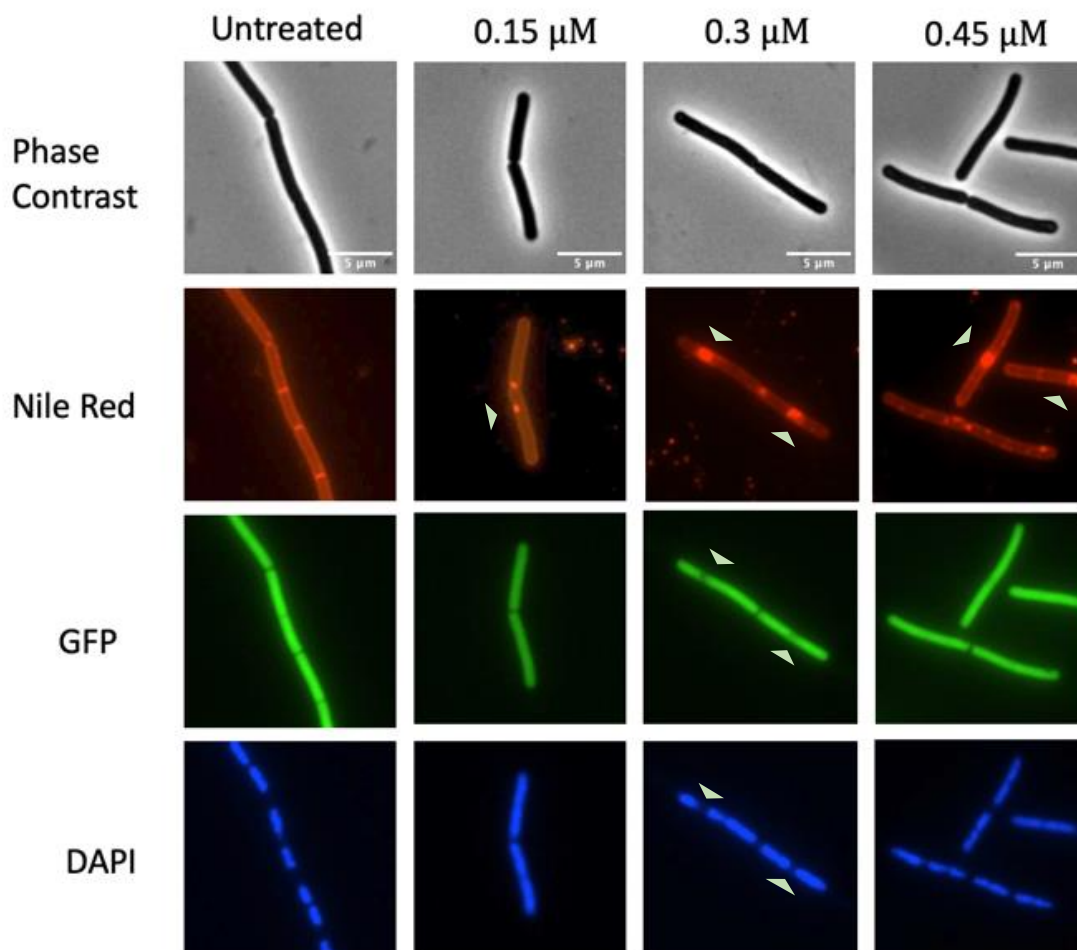


Figure 14. Bacterial Cytological Profiling of MW54 using Re4 with Nile red, GFP and DAPI stains

In Figure 14 the 0.3 μM concentration shows that the GFP signal is lacking in the same localization as the membrane blebs, showing an invagination effect of the compound. In untreated control cells, the DAPI stains showed a regular pattern with evenly sized and regularly distributed nucleoids, which indicates normal nucleoid packing and distribution in the cells. Furthermore, no signs of cell lysis or other morphological changes were observed in the phase contrast images.

4.1 Nucleoid Compaction Analysis

The graph obtained by performing nucleoid compaction analysis on OriginLab shows that not much difference is observed between Untreated growth control and the lowest concentration of Re1. However, interestingly the second and highest concentration shows significant difference when compared to the untreated growth control. It is also noticed that there is a bigger area of nucleoid, therefore, nucleoid is less compacted. The same was confirmed by comparing the data obtained by using a two-tailed student's t-test.

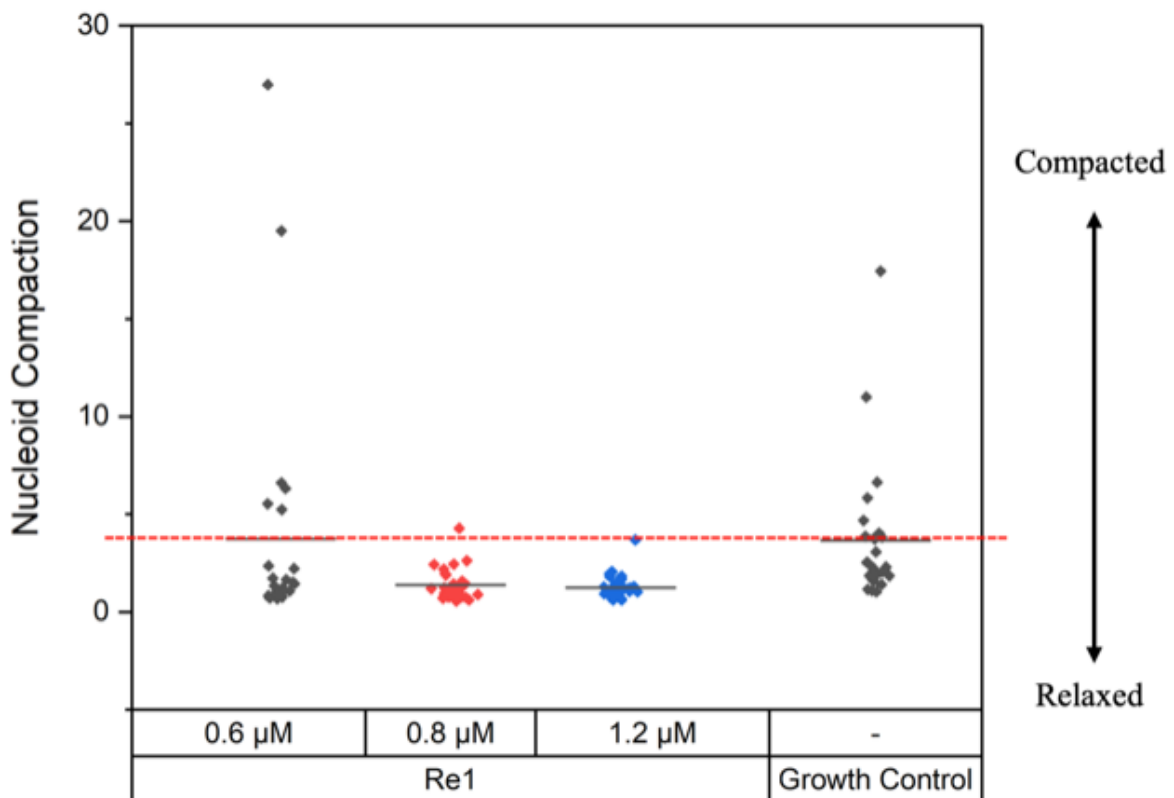


Figure 15. Nucleoid compaction measurement for Re1 with a Macro developed by Grimshaw. Measurements were done using DAPI channel of the BCP experiment of 3 biological replicates. Nucleoid compaction was calculated by the ratio of cell area and DNA area. A low value corresponds to a relaxed nucleoid, while a high value indicates higher DNA compaction. The median of the negative control is indicated with a dashed red line. The black dash indicates the median of the data set. Statistical significance was conducted using a two-tailed student's t-test ($p \leq 0,05$)

However, by comparing with the graph obtained by Re1, it was observed that in Re4 the growth control is not statistically much different from treated ones. The highest concentration shows higher compaction in comparison with the untreated control. The median of the concentrations confirm the relaxation of nucleoids observed in the microscopy images.

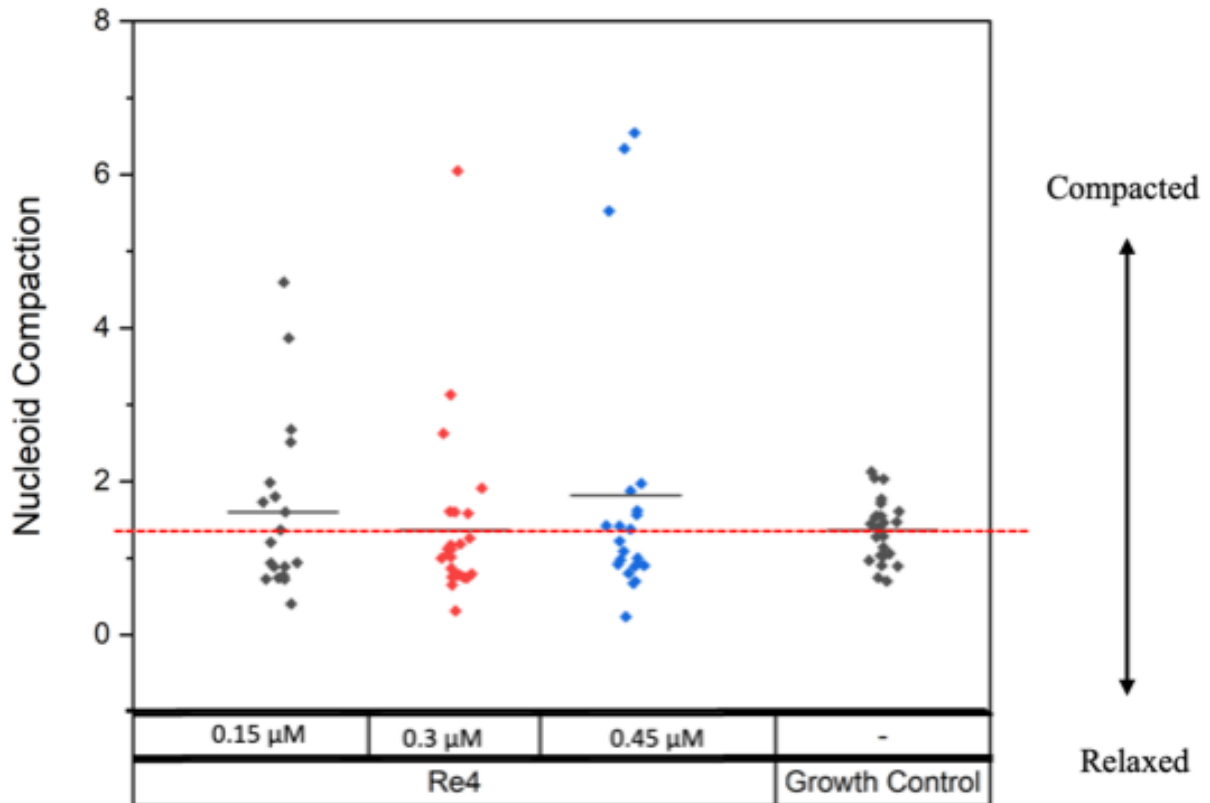


Figure 16. Nucleoid compaction measurement for Re4 with a Macro developed by Grimshaw. Measurements were done using DAPI channel of the BCP experiment of 3 biological replicates. Nucleoid compaction was calculated by the ratio of cell area and DNA area. A low value corresponds to a relaxed nucleoid, while a high value indicates higher DNA compaction. The median of the negative control is indicated with a dashed red line. The black dash indicates the median of the data set. Statistical significance was conducted using a two-tailed student's t-test ($p \leq 0,05$)

5. Protein Localization assay

5.1 *MinD* localization

MinD is a protein involved in the selection of the mid-cell division site in bacterial cells, and it plays a crucial role in the regulation of cell division. Specifically, MinD is part of the Min system, which is a set of proteins that helps to ensure proper placement of the division septum during cell division. The GFP allows to visualize and study sub-cellular localization, they from accumulations at mid-cells and protein is retained at newly formed poles. Here, gramicidin is used as a positive control as it is a polypeptide antibiotic that forms small pores in the cell membrane.

It was noted that since the cells treated with Re1 in DiSC₃(5) assay did not show depolarization occurring and hence by studying the images derived from MinD for Re1, it can be concluded that the results correlate with each other.

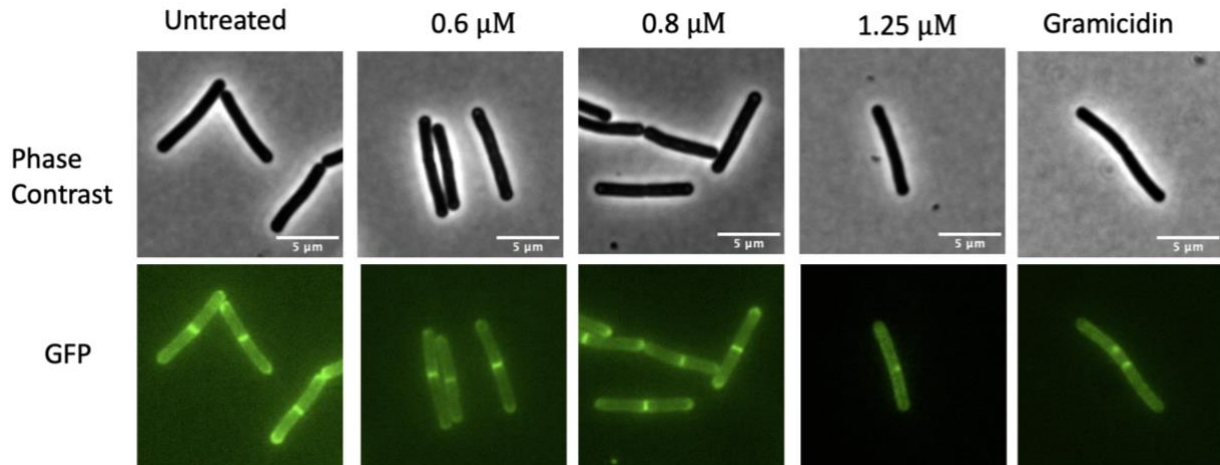


Figure 17. *MinD* localization for Re1 using GFP

On the other hand, the cells treated with Re4 in DiSC₃(5) assay did show depolarization occurring when the DiSC is added (figure 12).

In the images below (figure 18) the results do not correlate with the DiSC assay for Re4 as the cells do not look stressed. It could be the result of the 30 min antibiotic treatment that was given

to the cells before the microscopy assay and the cells would have recovered membrane potential.

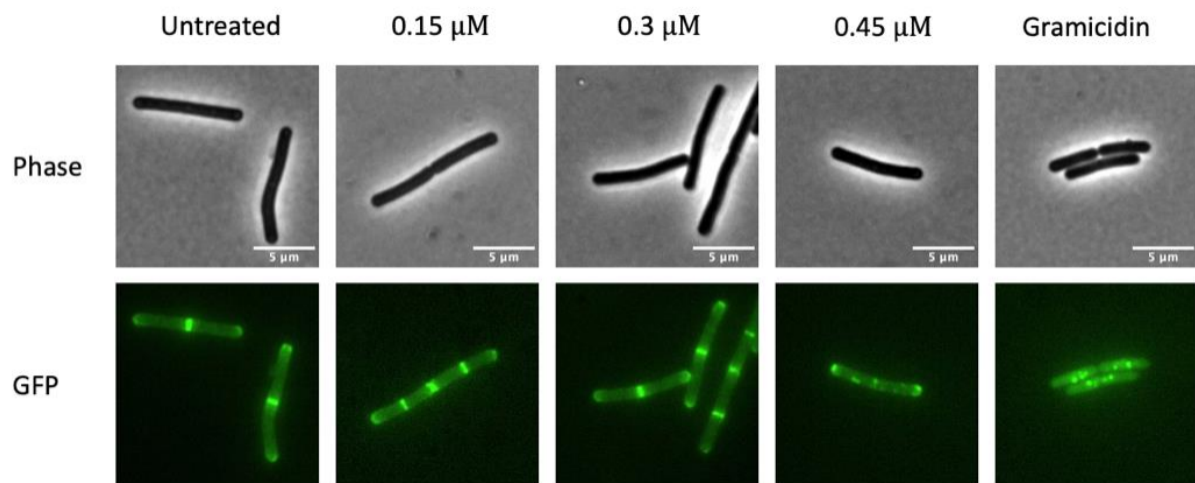


Figure 18. *MinD* localization for *Re4* using *GFP*

Therefore, another batch of cells were prepared and they were treated for 5 mins with the antibiotic since the peak in the DiSC graph could be seen at 5-10 mins. It can be seen in figure 19 that after the 5 min antibiotic treatment the cells look stressed and could not recover membrane potential which correlates with the DiSC results.

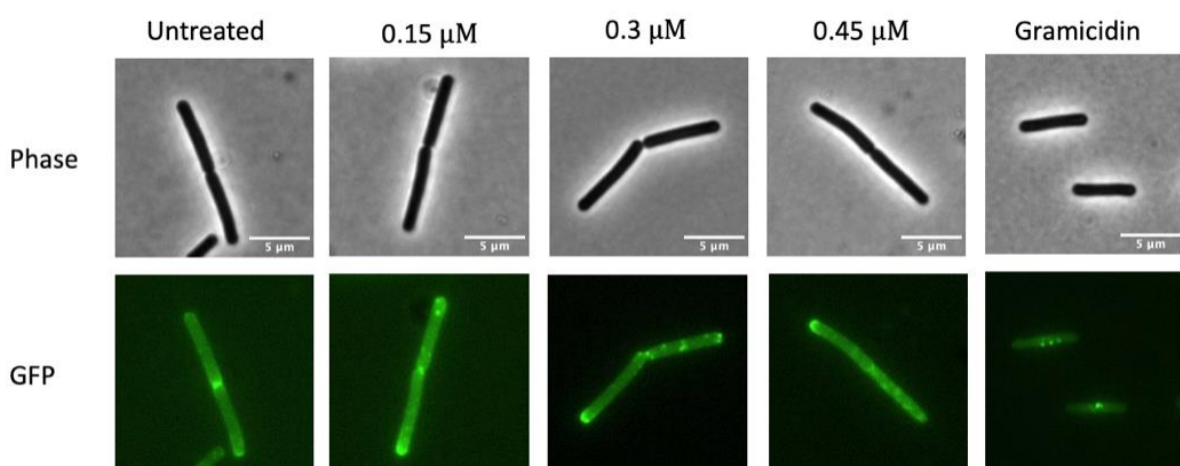


Figure 19. *MinD* localization for *Re4*(5 minute antibiotic treatment) using *GFP*

5.2 *RecA* localization

The RecA protein is involved in homologous recombination, which is a repair mechanism for DNA strand breaks. It is used to determine GFP protein involved in repair of DNA damage. By the subcellular localization of RecA under different concentrations, the DNA damage and repair mechanism can be known. The higher GFP signal represent a higher RecA expression, indicating that the compound is causing DNA damage. Here, Mitomycin C is used as a positive control as it binds to DNA which leads to cross-linking and inhibition of DNA synthesis and function. Under normal conditions, RecA is localized over the cytosol with a slightly brighter GFP signal over the nucleoid as seen in figure 20.

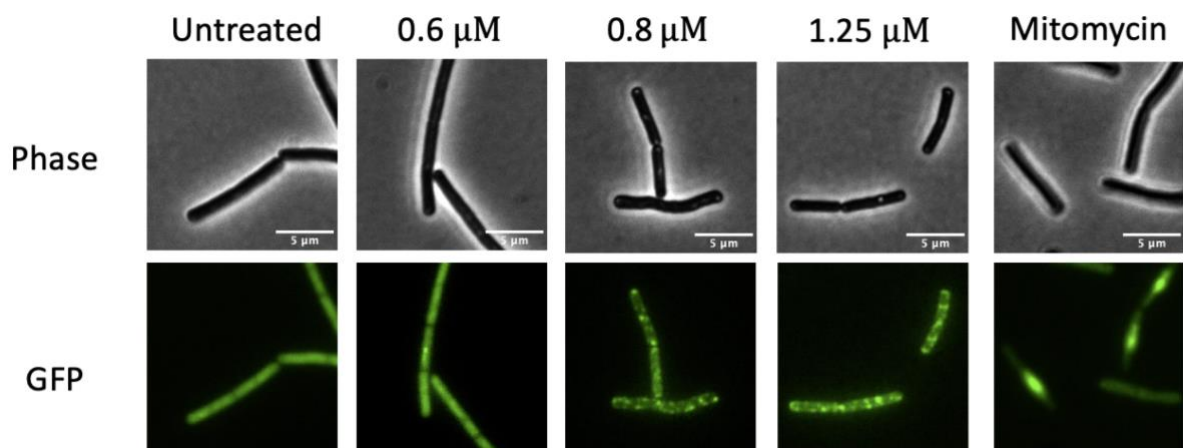


Figure 20. *RecA* localization for *Rel* using GFP

For cells treated with Re4 the higher concentrations are positive for DNA damage but not as significant as for Re1. This can be confirmed by checking the GFP signal which is not as brightly visible over the nucleoids in Re4 as compared to Re1

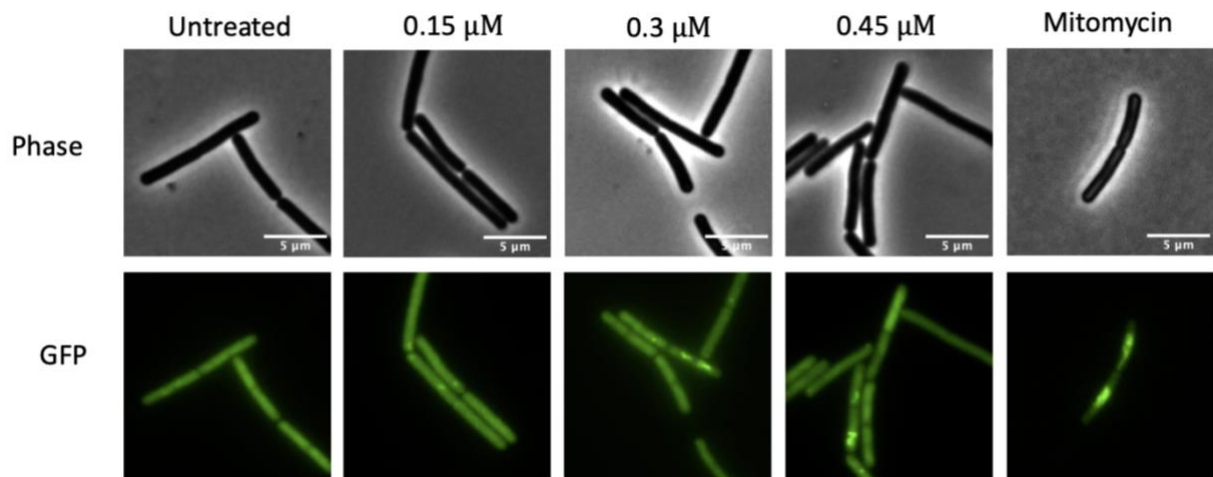


Figure 21. *RecA* localization for Re4 using GFP

5.3 *MreB* localization

MreB is a protein found in bacteria that plays a key role in cell shape and cell wall synthesis. It is often compared to the eukaryotic cytoskeleton protein actin, as *MreB* is involved in the maintenance of cell shape by directing the movement of peptidoglycan-synthesizing enzymes in the bacterial cell wall. *MreB* is tagged with green fluorescent protein (GFP), in order to track its localization and movement within bacterial cells. The images were taken in an interval of 30 seconds to check the movement of cell constituents overtime and merged. If no movement is observed it can be concluded that inhibition of cell wall synthesis has not taken place.

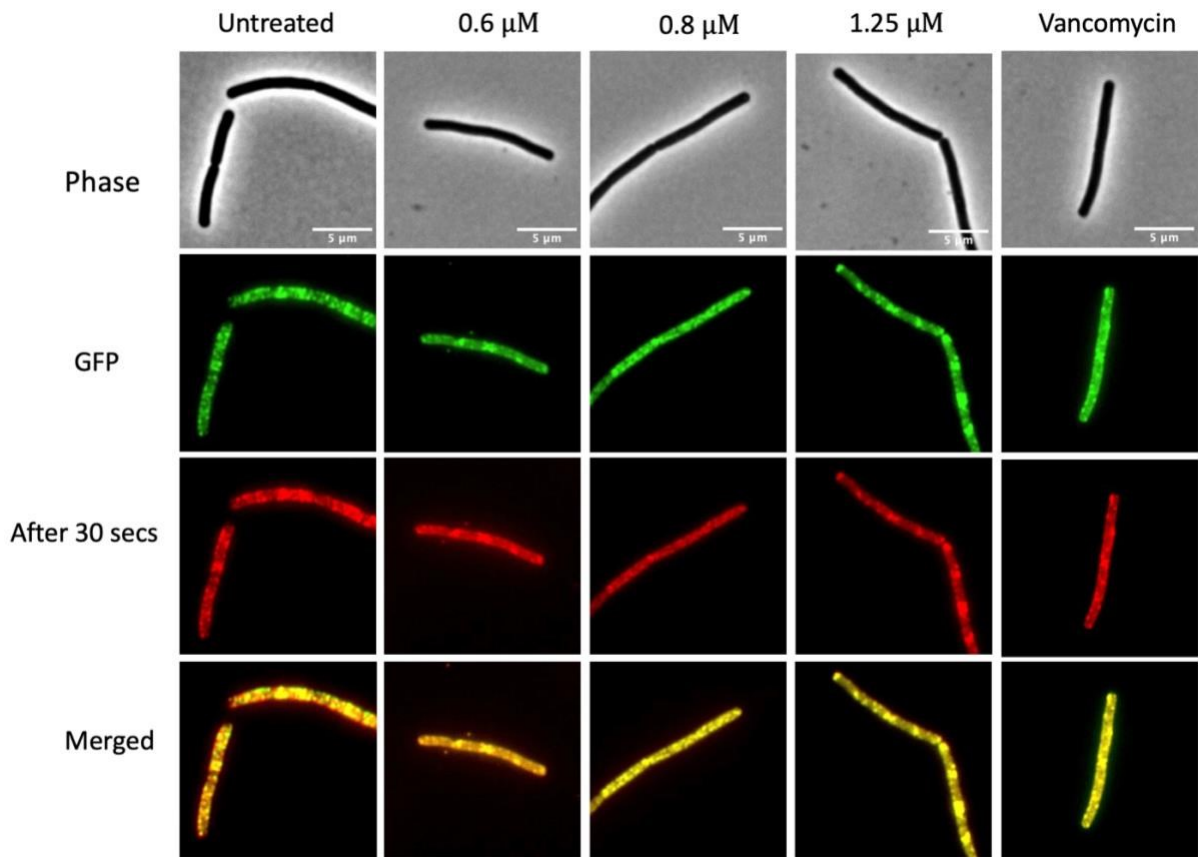


Figure 22. *MreB* localization for *Re1* using GFP

In both the cases, treatment with Re1 and Re4 both showed good movement as can be seen by merging GFP channel images before and after 30 seconds. This shows that there is non-inhibition of cell wall synthesis.

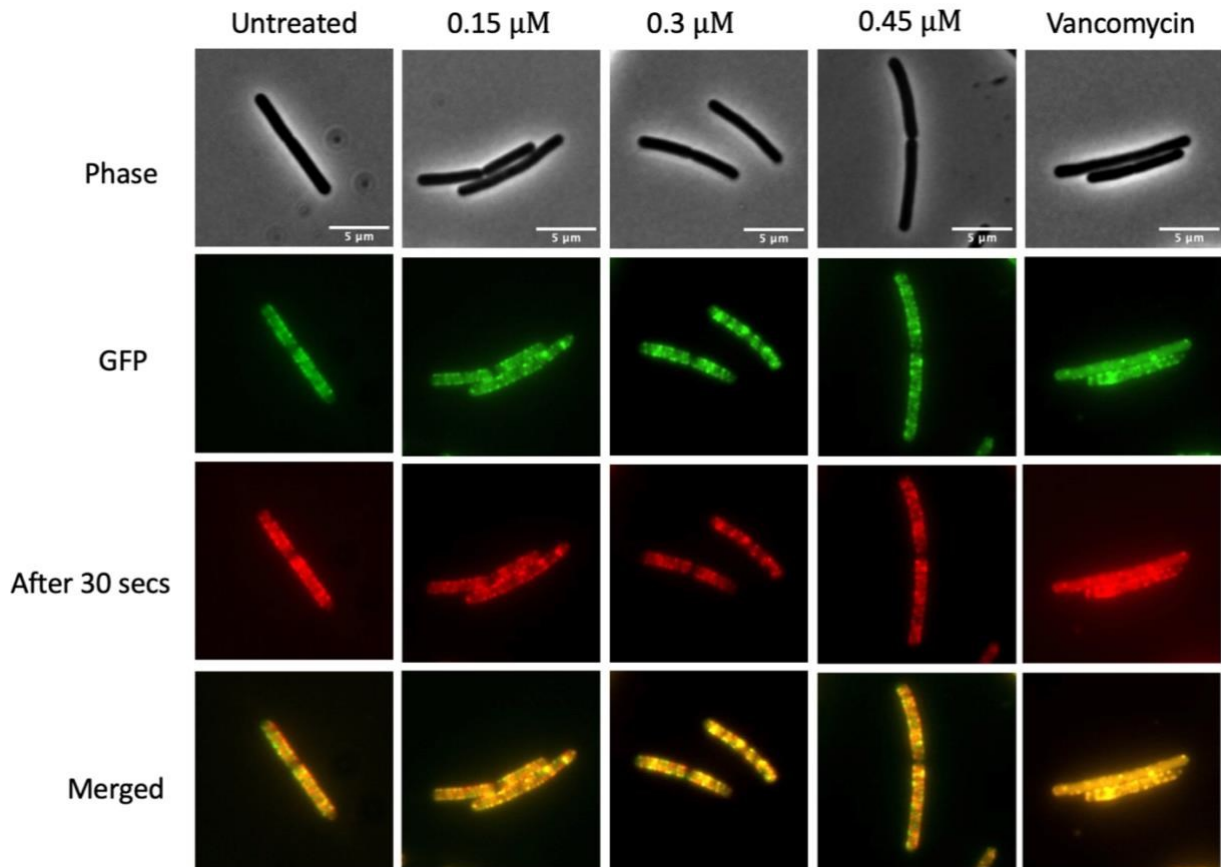


Figure 23. *MreB* localization for *Re4* using *GFP*

5.4 *DnaN* localization

DnaN is the beta-subunit of DNA polymerase III involved in the DNA replication process and helps in checking DNA condensation. It co-localizes with the nucleoids forming a pearl string-like structure. For *Re1* 0.8 μM shows round foci and the DNA arranged itself in a pearl string-like structure when compared with the untreated control. This could be due to DNA damage or DNA aggregation. Ciprofloxacin is used as a positive control as it is a bactericidal antibiotic of the fluoroquinolone drug class. It inhibits DNA replication by inhibiting bacterial DNA topoisomerase and DNA-gyrase (Shariati *et al.*, 2022) and condenses DNA in blobs.

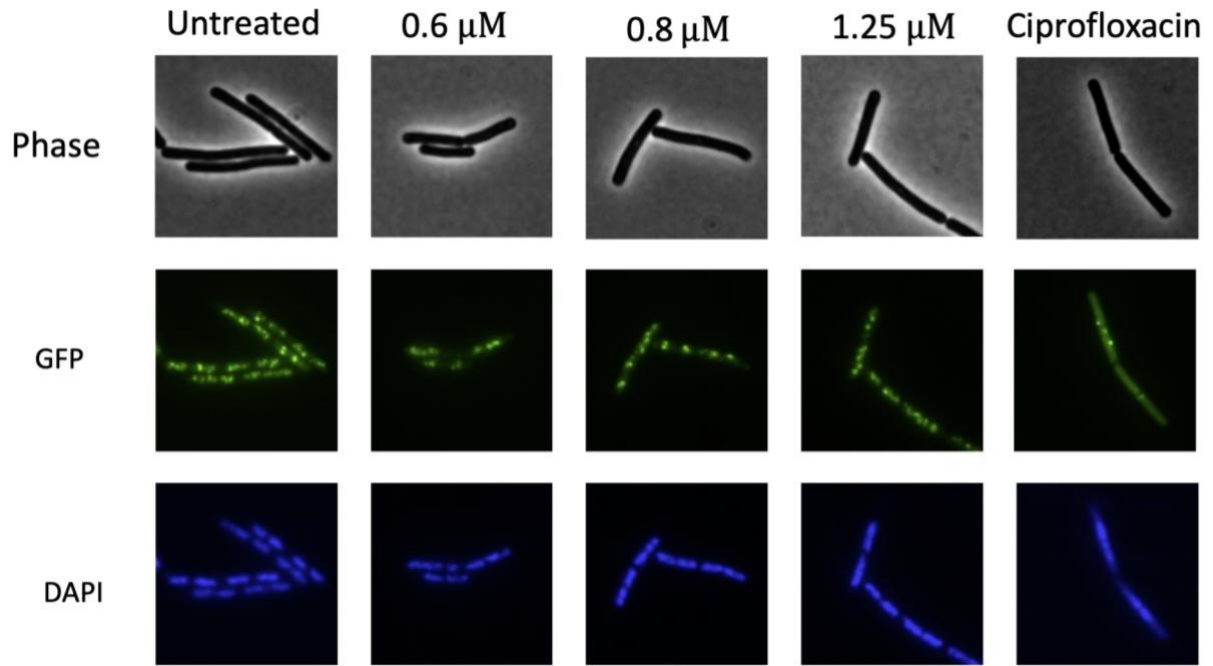


Figure 24. *dnaN* localization for Re1 using GFP and DAPI

For Re4, the blobs are more uniform and do not arrange in a pearl-string like structure.

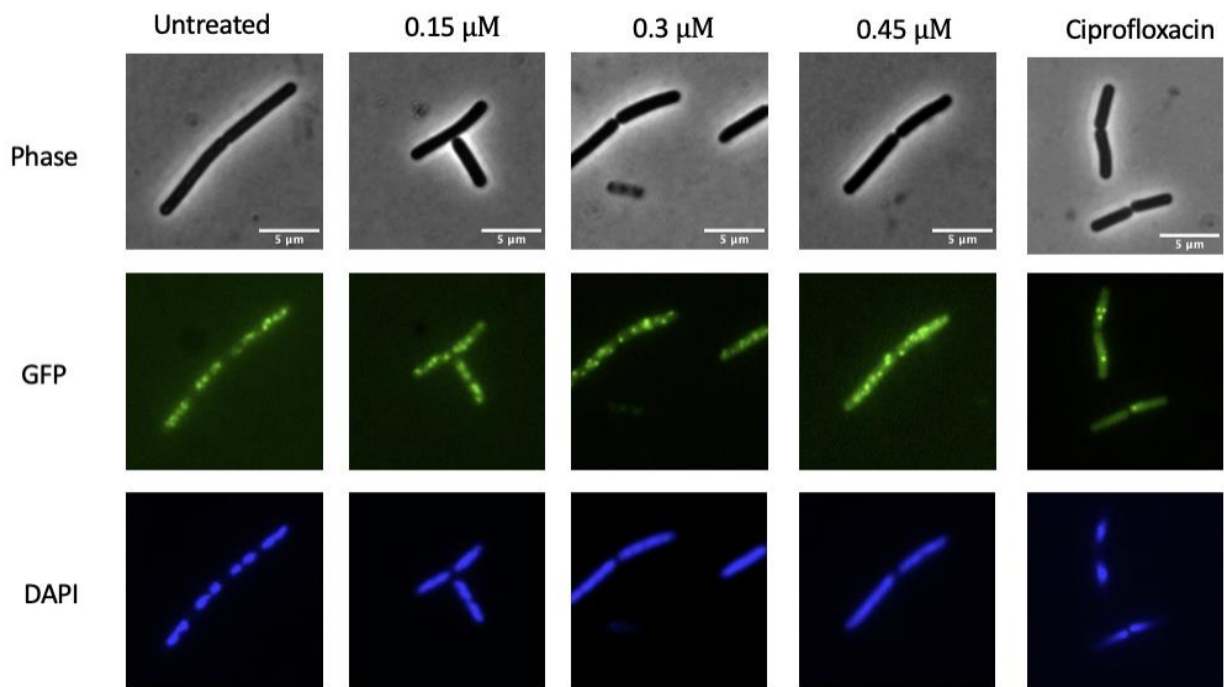


Figure 25. *dnaN* localization for Re4 using GFP and DAPI

The main difference seen in the above images is the agglomeration of the protein, and which is why it was decided to explore the YocM strain.

5.4 YocM localization

The YocM protein in *Bacillus subtilis* is identified as a small heat shock protein (sHsp) that plays a significant role in the organism's response to salt stress. It operates as part of the cellular protein quality control system, helping to protect the cells under conditions of heat or salt stress. YocM is involved in the localization to intracellular protein aggregates in response to salt and heat stress. This protein's function is crucial for the survival of *Bacillus subtilis* cells under stressful conditions, particularly in environments with high salt concentrations (Hantke *et al.*, 2019).

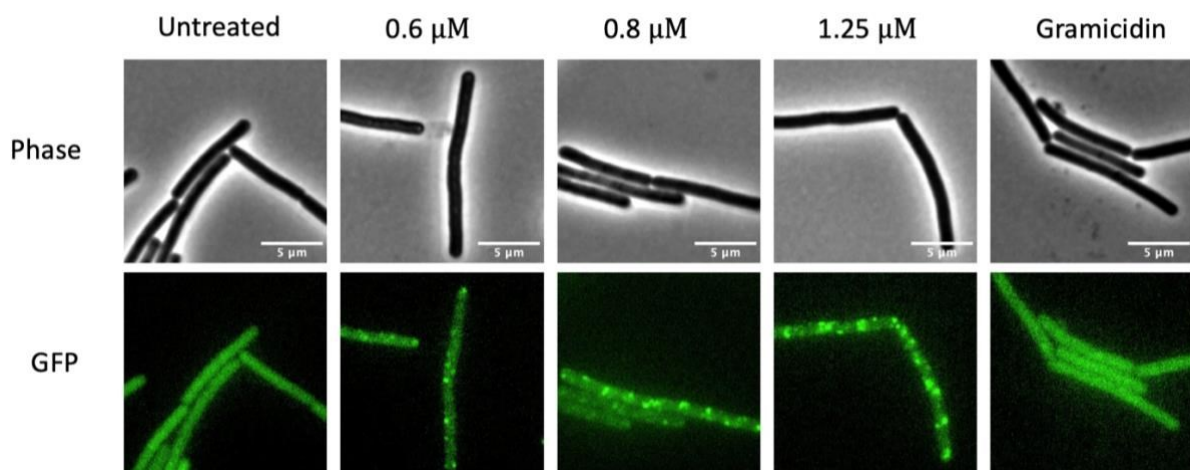


Figure 26. YocM localization for Rel using GFP

The above image shows presence of clusters, gradually increasing with the concentration, which shows positive for protein aggregation. According to the PhD thesis submitted by James Grimshaw, YocM, a reporter for protein aggregation, suggests that clustering is not induced by degradosome formation, but rather a novel, non-specific aggregation triggered by a decrease in cytoplasmic pH.

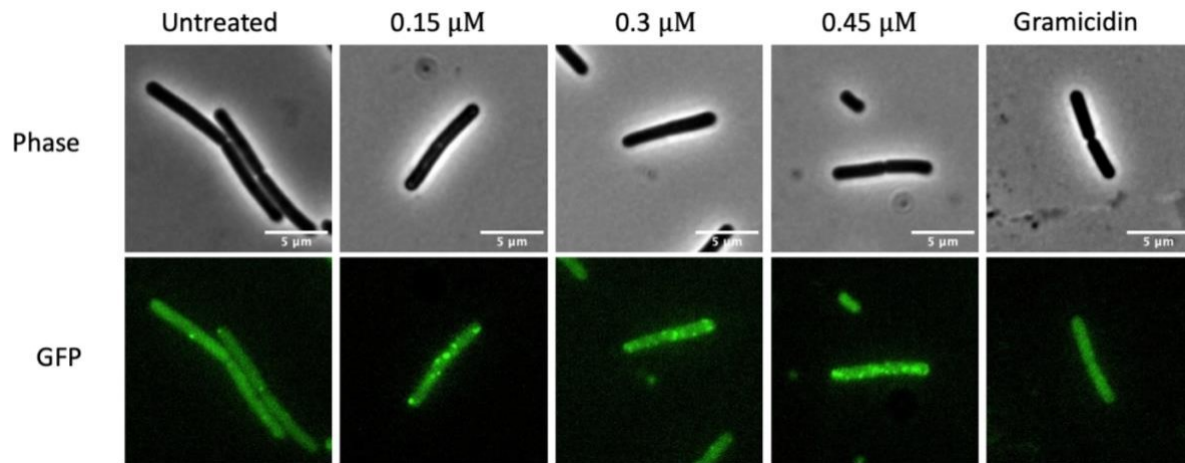


Figure 27 *YocM* localization for *Re4* using GFP

The above images show similar, concentration dependent results for *Re4*. The blobs signify presence of protein aggregation which is triggered by a decrease in cytoplasmic pH.

6. Single Molecule Localization Imaging

This assay was performed in collaboration with Fredrick Westerlund's (Head of Division at Chalmers University of Technology) group by Johanna Carlson.

When applied to the study of DNA repair, Single molecule localization can provide valuable insights into the dynamics of repair processes at the single-molecule level. To investigate DNA damage and repair mechanisms and to also understand the underlying cellular mechanism by using different concentrations of Re compounds to detect DNA lesions. The fluorophores attached to DNA repair markers helped in visualizing the repair events.

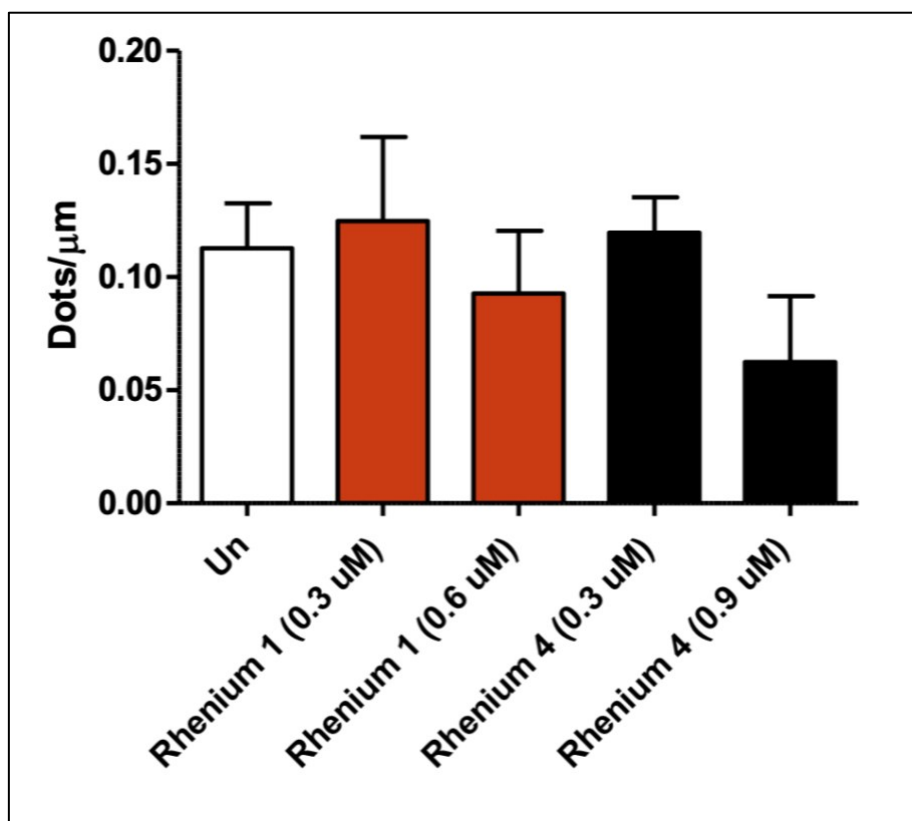


Figure 28 Highest and lowest concentration of Re1 and Re4 to perform single molecule imaging to check DNA damage repair

Here, by comparing both the rhenium compounds it can be said that there is not a vast difference between the DNA damage processes occurring inside the cells by treating with highest and lowest concentrations of Re1 and Re4 as compared to untreated. The assay, however, has limitations in detecting very small lesions and certain types of base damage without specific fluorophores or probes.

Conclusions

Recent investigations have shown that metal complexes, especially those containing rhenium and its many derivatives, have a great deal of promise as effective candidates for the creation of new antibiotics. Rhenium has become a focus of antimicrobial research due to its special chemical characteristics and adaptable coordination chemistry. It can be found in a wide range of complexes that have strong antibacterial effects on a variety of harmful microbes.

Studies on antimicrobials based on rhenium has highlighted how effective these compounds are at interfering with vital bacteria functions such as DNA connections, enzyme activities, and cell membrane integrity. These results demonstrate the several methods through which rhenium compounds function as antibacterial agents, offering a noteworthy benefit in the ongoing battle against antibiotic resistance.

Furthermore, rhenium complexes' structural tunability permits methodical alterations to improve their antibacterial capabilities. Researchers can adjust the pharmacokinetics and target specificity of these metal complexes by logically designing derivatives with particular ligands, coordination geometries, and electronic configurations. This tactical move makes it possible to tailor rhenium-based antibiotics to target the specific weaknesses of certain bacteria strains, opening the door to more focused and effective antimicrobial treatment.

To maximise the antibacterial potential of rhenium complexes, future research endeavours ought to concentrate on clarifying the structure-activity correlations of these compounds. Furthermore, investigating novel delivery methods and combinatorial strategies with currently available antibiotics may improve the overall effectiveness of antimicrobials based on rhenium. The development of next-generation antimicrobial drugs will be aided by the incorporation of sophisticated analytical techniques like spectroscopy and imaging, which will help to provide a thorough understanding of the interactions between these metal complexes and microbial targets.

In conclusion, the application of rhenium and related compounds as antimicrobials is a novel area of study for antibiotics. Antibiotic-resistant microorganisms constitute a growing threat to world health; yet, they can be effectively modified by planned alterations guided by structure-activity connections, as well as ongoing investigation of their specific features. The exploration of these pathways in subsequent studies will surely support the current endeavours to enlarge the stockpile of potent antibiotics and lessen the difficulties related to infectious illnesses.

References

1. Algammal, A.M. *et al.* (2020) 'Methicillin-resistant staphylococcus aureus (MRSA): One health perspective approach to the bacterium epidemiology, virulence factors, antibiotic-resistance, and zoonotic impact', *Infection and Drug Resistance*, 13. Available at: <https://doi.org/10.2147/IDR.S272733>.
2. Andrews, J.M. (2001) 'Determination of minimum inhibitory concentrations', *Journal of Antimicrobial Chemotherapy*, 48(SUPPL. 1). Available at: https://doi.org/10.1093/jac/48.suppl_1.5.
3. Baptista, P. V. *et al.* (2018) 'Nano-strategies to fight multidrug resistant bacteria-"A Battle of the Titans"', *Frontiers in Microbiology*. Available at: <https://doi.org/10.3389/fmicb.2018.01441>.
4. Bertranda, R.L. (2019) 'Lag phase is a dynamic, organized, adaptive, and evolvable period that prepares bacteria for cell division', *Journal of Bacteriology*. Available at: <https://doi.org/10.1128/JB.00697-18>.
5. Blumenthal, K.G. *et al.* (2019) 'Antibiotic allergy', *The Lancet*. Available at: [https://doi.org/10.1016/S0140-6736\(18\)32218-9](https://doi.org/10.1016/S0140-6736(18)32218-9).
6. Catalano, A. *et al.* (2022) 'Multidrug Resistance (MDR): A Widespread Phenomenon in Pharmacological Therapies', *Molecules*. Available at: <https://doi.org/10.3390/molecules27030616>.
7. Chawla, M. *et al.* (2022) 'Antibiotic Potentiators Against Multidrug-Resistant Bacteria: Discovery, Development, and Clinical Relevance', *Frontiers in Microbiology*. Available at: <https://doi.org/10.3389/fmicb.2022.887251>.
8. Claudel, M., Schwarte, J. V. and Fromm, K.M. (2020) 'New Antimicrobial Strategies Based on Metal Complexes', *Chemistry (Switzerland)*. Available at: <https://doi.org/10.3390/chemistry2040056>.

9. Collery, P., Desmaele, D. and Vijaykumar, V. (2019) 'Design of Rhenium Compounds in Targeted Anticancer Therapeutics', *Current Pharmaceutical Design*, 25(31). Available at: <https://doi.org/10.2174/1381612825666190902161400>.
10. Cooper, S.M. *et al.* (2022) 'Synthesis and anti-microbial activity of a new series of bis(diphosphine) rhenium(v) dioxo complexes', *Dalton Transactions*, 51(34). Available at: <https://doi.org/10.1039/d2dt02157a>.
11. Dadgostar, P. (2019) 'Antimicrobial resistance: implications and costs', *Infection and Drug Resistance*. Available at: <https://doi.org/10.2147/IDR.S234610>.
12. Davies, J. (1996) 'Origins and evolution of antibiotic resistance.', *Microbiología (Madrid, Spain)*. Available at: <https://doi.org/10.1128/membr.00016-10>.
13. Egorov, A.M., Ulyashova, M.M. and Rubtsova, M.Y. (2018) 'Bacterial enzymes and antibiotic resistance', *Acta Naturae*. Available at: <https://doi.org/10.32607/20758251-2018-10-4-33-48>.
14. Errington, J. and van der Aa, L.T. (2020) 'Microbe profile: Bacillus subtilis: Model organism for cellular development, and industrial workhorse', *Microbiology (United Kingdom)*, 166(5). Available at: <https://doi.org/10.1099/mic.0.000922>.
15. Evans, A. and Kavanagh, K.A. (2021) 'Evaluation of metal-based antimicrobial compounds for the treatment of bacterial pathogens', *Journal of Medical Microbiology*. Available at: <https://doi.org/10.1099/JMM.0.001363>.
16. Frei, A., Amado, M., *et al.* (2020) 'Light-Activated Rhenium Complexes with Dual Mode of Action against Bacteria', *Chemistry - A European Journal*, 26(13). Available at: <https://doi.org/10.1002/chem.201904689>.
17. Frei, A., Zuegg, J., *et al.* (2020) 'Metal complexes as a promising source for new antibiotics', *Chemical Science*, 11(10). Available at: <https://doi.org/10.1039/c9sc06460e>.

18. Frei, A. *et al.* (2023) 'Metals to combat antimicrobial resistance', *Nature Reviews Chemistry*. Available at: <https://doi.org/10.1038/s41570-023-00463-4>.
19. Gasser, G. (2015) 'Metal complexes and medicine: A successful combination', *Chimia*. Available at: <https://doi.org/10.2533/chimia.2015.442>.
20. Ghosh, S. (2019) 'Cisplatin: The first metal based anticancer drug', *Bioorganic Chemistry*. Available at: <https://doi.org/10.1016/j.bioorg.2019.102925>.
21. Hantke, I. *et al.* (2019) 'YocM a small heat shock protein can protect *Bacillus subtilis* cells during salt stress', *Molecular Microbiology*, 111(2). Available at: <https://doi.org/10.1111/mmi.14164>.
22. Kenny, R.G. and Marmion, C.J. (2019) 'Toward Multi-Targeted Platinum and Ruthenium Drugs - A New Paradigm in Cancer Drug Treatment Regimens?', *Chemical Reviews*. Available at: <https://doi.org/10.1021/acs.chemrev.8b00271>.
23. Kotrange, H. *et al.* (2021) 'Metal and metal oxide nanoparticle as a novel antibiotic carrier for the direct delivery of antibiotics', *International Journal of Molecular Sciences*. Available at: <https://doi.org/10.3390/ijms22179596>.
24. Lloyd, N.C. *et al.* (2005) 'The composition of Ehrlich's Salvarsan: Resolution of a century-old debate', *Angewandte Chemie - International Edition*, 44(6). Available at: <https://doi.org/10.1002/anie.200461471>.
25. Martens, K.J.A. *et al.* (2022) 'Enabling Spectrally Resolved Single-Molecule Localization Microscopy at High Emitter Densities', *Nano Letters*, 22(21). Available at: <https://doi.org/10.1021/acs.nanolett.2c03140>.
26. Mjos, K.D. and Orvig, C. (2014) 'Metallo drugs in medicinal inorganic chemistry', *Chemical Reviews*. Available at: <https://doi.org/10.1021/cr400460s>.

27. Morrison, C.N. *et al.* (2022) ‘Correction: Expanding medicinal chemistry into 3D space: metallofragments as 3D scaffolds for fragment-based drug discovery’, *Chemical Science*, 13(32). Available at: <https://doi.org/10.1039/d2sc90145e>.
28. Murugaiyan, J. *et al.* (2022) ‘Progress in Alternative Strategies to Combat Antimicrobial Resistance: Focus on Antibiotics’, *Antibiotics*. Available at: <https://doi.org/10.3390/antibiotics11020200>.
29. Nandhini, P. *et al.* (2022) ‘Recent Developments in Methicillin-Resistant Staphylococcus aureus (MRSA) Treatment: A Review’, *Antibiotics*. Available at: <https://doi.org/10.3390/antibiotics11050606>.
30. Nonejuie, P. *et al.* (2013) ‘Bacterial cytological profiling rapidly identifies the cellular pathways targeted by antibacterial molecules’, *Proceedings of the National Academy of Sciences of the United States of America*, 110(40). Available at: <https://doi.org/10.1073/pnas.1311066110>.
31. Pedreira, T., Elfmann, C. and Stülke, J. (2022) ‘The current state of SubtiWiki, the database for the model organism *Bacillus subtilis*’, *Nucleic Acids Research*, 50(D1). Available at: <https://doi.org/10.1093/nar/gkab943>.
32. Ramotowska, S. *et al.* (2020) ‘A comprehensive approach to the analysis of antibiotic-metal complexes’, *TrAC - Trends in Analytical Chemistry*. Available at: <https://doi.org/10.1016/j.trac.2019.115771>.
33. Reham Z. Hamza *et al.* (2022) ‘Efficacy of some antibiotics and some metal complexes (Nano-formula) that could increase their effectiveness during COVID-19’, *International Journal of Biological and Pharmaceutical Sciences Archive*, 3(1). Available at: <https://doi.org/10.53771/ijbpsa.2022.3.1.0021>.

34. Saeloh, D. *et al.* (2018) 'The novel antibiotic rhodomyrton traps membrane proteins in vesicles with increased fluidity', *PLoS Pathogens*, 14(2). Available at: <https://doi.org/10.1371/journal.ppat.1006876>.
35. Salam, M.A. *et al.* (2023) 'Antimicrobial Resistance: A Growing Serious Threat for Global Public Health', *Healthcare (Switzerland)*. Available at: <https://doi.org/10.3390/healthcare11131946>.
36. Sánchez-López, E. *et al.* (2020) 'Metal-based nanoparticles as antimicrobial agents: An overview', *Nanomaterials*. Available at: <https://doi.org/10.3390/nano10020292>.
37. Schäfer, A.B. and Wenzel, M. (2020) 'A How-To Guide for Mode of Action Analysis of Antimicrobial Peptides', *Frontiers in Cellular and Infection Microbiology*. Available at: <https://doi.org/10.3389/fcimb.2020.540898>.
38. Shariati, A. *et al.* (2022) 'The resistance mechanisms of bacteria against ciprofloxacin and new approaches for enhancing the efficacy of this antibiotic', *Frontiers in Public Health*. Available at: <https://doi.org/10.3389/fpubh.2022.1025633>.
39. Sharifi-Rad, M. *et al.* (2020) 'Lifestyle, Oxidative Stress, and Antioxidants: Back and Forth in the Pathophysiology of Chronic Diseases', *Frontiers in Physiology*. Available at: <https://doi.org/10.3389/fphys.2020.00694>.
40. Sharma, B. *et al.* (2022) 'Antimicrobial Agents Based on Metal Complexes: Present Situation and Future Prospects', *International Journal of Biomaterials*. Available at: <https://doi.org/10.1155/2022/6819080>.
41. Siegmund, D. *et al.* (2017) 'Benzannulated Re(i)-NHC complexes: Synthesis, photophysical properties and antimicrobial activity', *Dalton Transactions*, 46(44). Available at: <https://doi.org/10.1039/c7dt02874a>.

42. Snezhkina, A. V. *et al.* (2020) ‘ROS generation and antioxidant defense systems in normal and malignant cells’, *Oxidative Medicine and Cellular Longevity*. Available at: <https://doi.org/10.1155/2019/6175804>.
43. Sovari, S.N. *et al.* (2020) ‘Design, synthesis and in vivo evaluation of 3-aryl coumarin derivatives of rhenium(I) tricarbonyl complexes as potent antibacterial agents against methicillin-resistant *Staphylococcus aureus* (MRSA)’, *European Journal of Medicinal Chemistry*, 205. Available at: <https://doi.org/10.1016/j.ejmech.2020.112533>.
44. Vatansever, F. *et al.* (2013) ‘Antimicrobial strategies centered around reactive oxygen species - bactericidal antibiotics, photodynamic therapy, and beyond’, *FEMS Microbiology Reviews*. Available at: <https://doi.org/10.1111/1574-6976.12026>.
45. Wenzel, M. *et al.* (2018) ‘Assessing Membrane Fluidity and Visualizing Fluid Membrane Domains in Bacteria Using Fluorescent Membrane Dyes’, *BIO-PROTOCOL*, 8(20). Available at: <https://doi.org/10.21769/bioprotoc.3063>.
46. te Winkel, J.D. *et al.* (2016) ‘Analysis of antimicrobial-triggered membrane depolarization using voltage sensitive dyes’, *Frontiers in Cell and Developmental Biology*, 4(APR). Available at: <https://doi.org/10.3389/fcell.2016.00029>.
47. Zalejski, J., Sun, J. and Sharma, A. (2023) ‘Unravelling the Mystery inside Cells by Using Single-Molecule Fluorescence Imaging’, *Journal of Imaging*, 9(9). Available at: <https://doi.org/10.3390/jimaging9090192>.
48. Zhang, P. and Sadler, P.J. (2017) ‘Redox-Active Metal Complexes for Anticancer Therapy’, *European Journal of Inorganic Chemistry*. Available at: <https://doi.org/10.1002/ejic.201600908>.